AIT

Asian Institute of Technology
Thailand

thesis No. RS - 09 - 06

EXTRACTION OF MANGROVE FOREST PARAMETERS USING AIRBORN LIDAR FOR TSUNAMI RUN-UP MODEL

Wasinee Cheunban

EXTRACTION OF MANGROVE FOREST PARAMETERS USING AIRBORN LIDAR FOR TSUNAMI RUN-UP MODEL

by

Wasinee Cheunban

A thesis submitted in partial fulfillment of the requirements for the degree of Master of Science in
Remote Sensing and Geographic Information Systems

Examination Committee: Dr. Kiyoshi Honda (Chairperson)
Prof. Seishiro Kibe
Dr. Phisan Santitamnont
Dr. Wataru Ohira

Nationality: Thai
Previous Degree: Bachelor of Science in Geography
Kasetsart University
Bangkok, Thailand

Scholarship Donor: Royal Thai Government
National Center for Genetic Engineering and Biotechnology (BIOTEC), Thailand

Asian Institute of Technology
School of Engineering and Technology
Thailand
May 2009

Abstract

In this thesis research, Canopy Height Model (CHM) deriving from LiDAR was employed to extract the essential parameters of mangrove tree attributions at individual tree scale e.g. tree top, tree height and crown width. The investigation of the relationship of tree crown and tree height from ground inventory leads to the implement of linear regression which was used to specify the circular window size to estimate tree apex, tree height and crown width from CHM. The comparisons of estimated value and ground truth were established. RMS error and relevant statistic were considered. Consequently, to fulfill the Tsunami simulation model for calculation of the resistance force, effective stem volume and projected area under water level are the critical parameters. Trunk shape functions based on Komiyama model were implemented to calculate stem volume and projected area of mangrove tree at each water depth. To validate the estimated volume, the results deriving from Komiyama must be equal to the integration volume obtaining from trunk shape function. Besides, DBH from function R(x) have to equal DBH from field survey.

The results reveal that the relationship of tree height and crown diameter from field inventory is rather positive explained by linear regression with high coefficient correlation R^2 (0.791). TreeVaW is capable to extract mangrove forest parameters from Canopy Height Model (CHM) deriving from LiDAR with RMS error of 0.155m, 0.29m, 0.599m, 0.781cm according to tree location in X, location in Y , tree height and crown width respectively. Consequently, the investigation of the strong relationship between DBH, tree height and crown width from the field ($R^2 = 0.91$) leads to the construction of DBH model that can be used to estimate DBH from tree height and crown width from LiDAR. To validate the model, estimated DBH was compared with the observed DBH resulting in the positive with R^2 of 0.819. To simulate Tsunami run-up model, trunk diameter function for simulating the tree trunk shape and calculating the attributes of mangrove tree was developed and investigated based on the assumption of cylinder model and $R(x) = ax^b$ model. The examination of results express that trunk diameter function has a potential to calculate trunk volume and projected are under water level. Following outcomes will be further used to calculate the resistant force against Tsunami wave in the Tsunami run-up model.

ACKNOWLEDGEMENTS

The success of this thesis would have not been possible without the assistant and cooperation of many persons and organization. First of all, I wish to communicate my gratitude to Dr. Kiyoshi Honda who facilitates and provides constructive suggestions to my thesis research. Many thanks for his enthusiasm to find the solution to solve trunk diameter functions. He is very nice teacher especially in crisis situation.

I wish to reveal my gratitude to Prof. Seishiro Kibe who makes clearly for complicated equation and endeavor to complete that accepts to be my thesis committee.

My very grateful is conveyed to Dr. Phisan Santitamnont that provides me with LiDAR data and technical suggestions as well as to Dr. Wataru Ohira that gives me some ideas about Tsunami run-up model.

Special thanks are given to Dr. Sorin C. Popescu from Texas A&M University who support the source code for TreeVaW and to Dr. Sasitorn Poungparn from Chulalongkorn University who explain the details of Komiyama model.

I appreciate the generous partial financial support extended to me from the Royal Thai Government (RTG) and my organization (BIOTEC) that responds for the remaining scholarship as well as BRT that supports the research budget.

I am deeply indebted to my family for all their help. Also I wish to express my grateful to Mr.Poonsak Miphokasap, my classmates, my seniors and my juniors in RS&GIS FOS.

Last but not least, I wish express my strong and sincere gratitude to me for my enthusiasm, my concentration and my engrossment to accomplish an arduous task.

TABLE OF CONTENS

TABLE OF CONTENS (CONT.)

LIST OF TABLES

LIST OF FIGURES

CHAPTER I

INTRODUCTION

1.1 Background

Thailand is situated in equator zone usually countering with various violent disasters. In recent years, severe disasters e.g. hurricane, flood, earthquake, Tsunami are concerned as the global issue affected in the large scale. The impacts have many critical consequences on the various ecosystems from high mountainous to lowland plain as well as in the coastal region. In 2004, many countries along the coastal had been affected by Tsunami storm surf with the wave of 5-10m. As a result of disasters, natural resources, man-made infrastructures as well as human life were damaged suddenly. Tsunami is the long-wavelength and long-period sea waves caused by the effects of large magnitude of earthquake under the deep ocean that produces the sudden or abrupt movement of large volumes of water. Unfortunately, Thailand also is placed in the region of fault plane and Tsunami effects. It means that the rigid phenomena are possibly repeated. To avoid the crisis experience, the knowledge and understanding of Tsunami is essential for closed monitoring, mitigation, prevention and management.

K. Harada et al. (2002) had been realized that mangrove and costal forest inter tidal wetlands and forming important marine ecosystem would be utilized as natural tool to be effective buffer against impact of the natural hazards composing of enormous wave. The fringing mangrove along the coastline can reduce the power of the rigorous wave and the loss of life. To reduce the impacts of Tsunami, detailed data and information of mangrove forest are needed to be established and identified the situation and prevention action plan. Hydraulic resistance and reflection of trees could reduce Tsunami energy, inundation depth, inundating area, current and hydraulic force behind the forest. K. Harada et al (2002) studied the mangrove control forest to reduce Tsunami impact in Japan. The experimental and numerical delineation to understand a dynamic behavior of Tsunami passing through a mangrove forest and to evaluate its effectiveness as Tsunami control forest were conducted.

In general, the concept of Tsunami model is focusing on the endeavor to understand its effect, planning for land use, conservation and cultivation of forest. Effect estimation of Tsunami is required for proper understanding of the contribution of forest on Tsunami disaster mitigation. To implement the potential Tsunami model, the quality and quantity of mangrove to reduce attacking wave must be evaluated and formulated, so that the guidance of disaster mitigation will be performed. In this scenario, the input parameters are required for Tsunami mitigation model generally consisting of an accurate inventory of tree shape and tree parameter such as crown width, tree density, DBH (diameter at breast height), tree height, trees volume and basal area. Deriving quantitative measurements of mangrove attributes is the laborious task. In fact, mangrove areas are usually difficult to access due to the dense canopy and instable ground within the tidal zone. Which technology can be possibly utilized to achieve following information but still keeping high accuracy, time saving and updating is the challenging issue in this scenario.

1.2 Statement of problems

Due to the limitation of ground data acquisition in mangrove region, Geo-spatial technology that can capture the meaningful data along the coastal is promoted. Usually, it consists of Geographic Information System (GIS), Remote Sensing (RS) and Global Positioning System (GPS). With the advantages of this technology, wide scale data capture, near real-time monitoring, spatial data management and decision support system is capable to establish.

In Thailand, existing GIS data and satellite image is developed in several scales. But some of them are out-of-date owing to the expensive cost or limitation of technology. On the other hand, natural disaster like Tsunami is a dynamic system. Therefore, updating information is needed. High-resolution satellite images or color aerial photographs offer a cost-effective alternative to map the large scale and area of mangroves and some parameters can later be extracted. However, the main obstacles of an optical remote sensing for mangrove forest monitoring are the cloud contaminate particularly in monsoon season. In addition, the reflectance in spectral signatures for different mangrove forests is not distinctive in some cases and some information can not be achieved from 2D optical image. Therefore, passive remote sensing that detecting the surface objects by utilizing radar pulse becomes the new option to achieve the meaningful information in all situations, day and night, dry and rainy. Passive image generally have the several kinds relying on the platform, space borne or airborne. LiDAR known as LiDAR (Light Detection and Ranging) is fast becoming the preferred acquisition technique for forest canopy. In addition to providing a characterization of ground topography, LiDAR data give new information about the canopy surface and vegetation parameters, such as height, stem density, and crown dimension. Airborne laser mapping technology that increase another dimension in height for measuring mangrove attributes by offering accurate three dimensional profiles without the logistical difficulties of extensive ground surveys should be deem (M. A. Lefsky, 2002). LiDAR sensor allows scientists to analyze forests in a three-dimensional format over large areas.

Recently, LiDAR widely is utilized as the source of mangrove forest attributes. Subsequently, this information becomes the inputs of Tsunami resistant model. Previous studies that focused on estimating forest stand characteristics with LiDAR in plot level can be found in Harding et al., 1994; Lefsky et al., 1997, 1999; Weishampel et al., 1997; Blair et al., 1999; Means et al., 1999. However, the research focusing on the procedure to extract mangrove parameter through LiDAR is not popular particularly in an individual tree level. Presumably, different species of mangrove, different structure model is constructed. To develop the complete Tsunami model, the implement of process for parameter delineation and estimated model must be considered at first.

1.3 Research problems

(1) How to extract the essential mangrove forest parameters (tree position, tree height, crown width, DBH) from the LiDAR?

(2) How to estimate trunk volume and projected area at each height level?

1.4 Research objectives

(1) To extract the essential mangrove forest parameters, tree height, crown width and DBH, based on an individual tree crown from LiDAR,

(2) To implement the solution for calculating the trunk volume and projected area under water level.

1.5 Scope and limitation

The optimum goals of this study are to extract forest parameters from LiDAR at individual tree scale and to fulfill the Tsunami simulation model by estimating trunk volume and projected area under water level. LiDAR is the main source of elevation acquisition which corresponds to latitude, longitude and surface height. This research endeavors to make a contribution to the forest biophysical parameter extraction using LiDAR. The conceptual framework of research can be summarized following.

The first scenario was concentrated on the derivative of tree canopy height model (CHM) through LiDAR. To do so, digital elevation model (DEM) and digital surface model (DSM) must be constructed by taking an advantage of the last and first return respectively. The computation of DEM can be classed as two phases. The first phase involves the generation of DEM from the raw elevation points. In the second phase, certain interpolation based on the local minima is employed to generate the final DEM surface. In parallel, the first return LiDAR points were interpolated by linear method to generate DSM. Subsequently, the DSM and the DEM are subtracted to further produce the CHM.

The second scenario was devoted for parameter extraction from CHM. Initially, the relationship between crown width and tree height from field was investigated by linear regression. Then, relationship was used to specify the circular window size to compute tree apex, height and crown width. To do forth, TreeVaW, a versatile tool for analyzing forest canopy LiDAR was utilized. The estimated outputs were compared with the data from ground inventory. RSM error, statistics and accuracy were evaluated.

In the last scenario, the relationship of tree height, crown width and DBH from ground inventory will be used to reckon the DBH algometric Model. Trunk diameter function was constructed to derive the critical constant value a and b that capable to explain shape and size of tree trunk attributes corresponding to tree height. With the incorporation of estimated DBH, constant a and b, tree trunk volume and projected area along the interval 0.5m of water depth or tree height was feasibly to calculate. Trunk volume and projected area functions were implemented based on the Komiyama volume model.

1.6 Expected output

1. Mangrove forest parameters extracted from LiDAR at individual tree scale including:
    (1) Trees location
    (2) Tree height
    (3) Crown width
    (4) DBH (deriving from DBH model)
2. Estimation trunk volume and projected area under water level

1.7 Study area

The study site is located at Bang Poo sub-district (Tambon) along the coastline of Samutpakarn province, Thailand. Location map of Bang Poo is illustrated in Fig 1.1. The study area is approximately 100m x 100m. This region includes the dense mangrove forest in various stages of similar tree species (*Avicennia marina*). This study area is a flat in a tidal and mud zone with the mean elevation less than 1m. The surrounding of mangrove plot are many shrimp farm and factory.

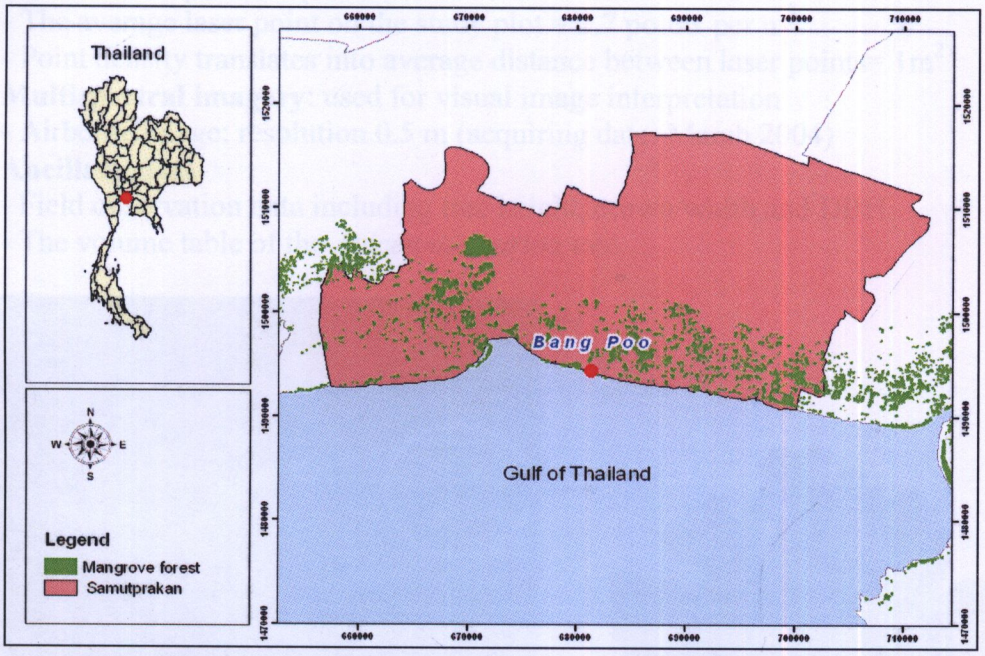

Figure 1.1 The study area at Bang Poo region, Samutprakan province and the distribution of mangrove forest extracted from Landsat image in 2008

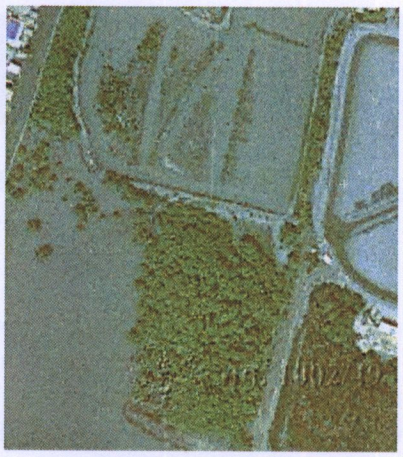

Figure 1.2 The mangrove forest survey plot 100m x 120 m within the study site

1.8 Materials and equipments

- **LiDAR dataset**
  - Acquiring date: June, 2005 during 9 – 12 a.m.
  - System: Optech Airborne Laser Terrain Mapper (ALTM) 2050

- Operator: LaserMap GPR Consultants of Canada, Royal Thai Survey Department and Chulalongkorn University
- Accuracy: horizontal 50 cm, vertical 10 cm
- Scanning Frequency Rate = 28 Hz
- Laser Repetition Rate = 50 kHz
- High of Flight = 1,000 meters
- Swath width = 750 meters
- Scanning Angle = 0^{o} to $\pm 20^{o}$
- Two returns per laser pulse: first and last
- The average laser point on the study plot = 2.7 points per m^2
- Point density translates into average distance between laser points= $1m^2$

- **Multispectral imagery**: used for visual image interpretation
  - Airborne image: resolution 0.5 m (acquiring date: March 2004)
- **Ancillary data**
  - Field observation data including tree height, crown width and DBH
  - The volume table of the *Avicennia marina* tree.

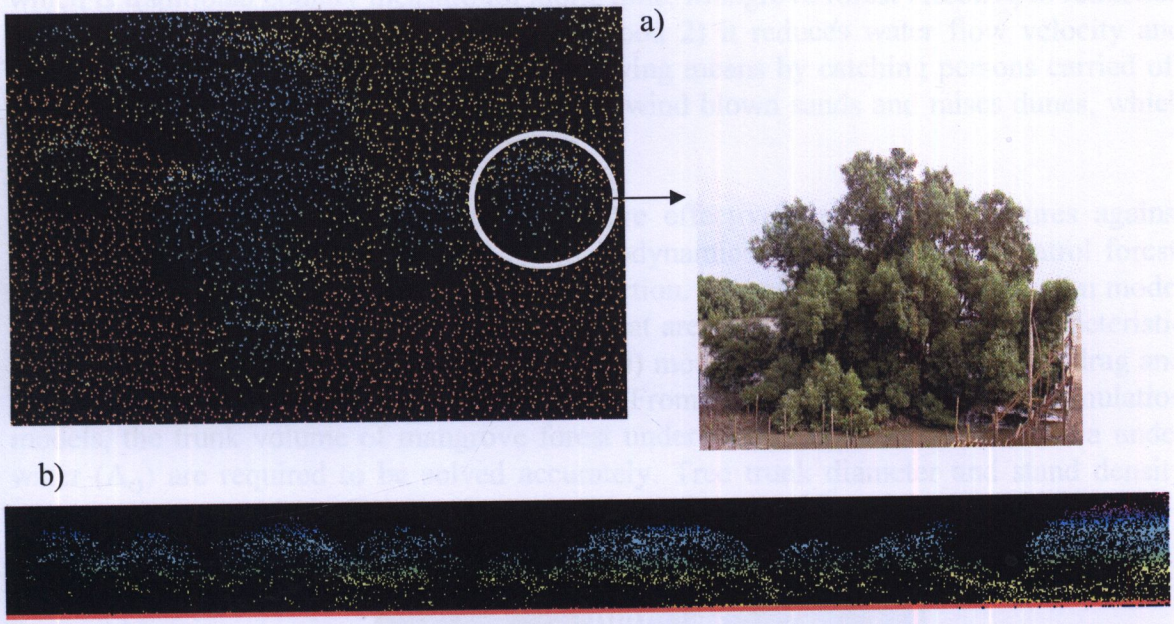

Figure 1.3 Vertical profile of LiDAR data a) the LiDAR image on the top view and b) LiDAR image on the front of the view

- **Softwares**
  - Image processing and GIS software: Envi4.3, ERDAS Image 9.2, ArcGIS.
  - LiDAR interpretation software: Point Value.
  - Tree height and crown radius extraction: Tree Variable Window program (TreeVaW), free public source code developed by Sorin Popescu, Texas A&M University with IDL language.
- **Ground survey equipments**
  - Diameter tape and distance tape
  - Handheld GPS
  - Handheld Haga altimeter
  - Rope
  - Label tag

CHAPTER II

LITERATURE REVIEWS

2.1 Tsunami and mangrove forest protection

2.1.1 Background

Nowadays, the natural disasters are an important world problem. After the tremendous Tsunami in many countries in 2004, it increases more the interesting of the protection and reduction of the disaster damages. The artificial coastal barriers needed high cost of the construction and maintenance change the present environment and have forced inconvenient to use the coastal area. Therefore, the countermeasures against Tsunami by using the artificial coastal barriers are not recommended for all coastal areas. It is required that a new countermeasures corresponding to every area is considering with the natural functions for more appropriate management for natural disaster reduction and keeping good environment. One of a new way to achieve that is to utilize control forest along coast which is traditional counter measure for along time. Mangrove forest effective to reduction of Tsunami energy because 1) it stops driftwood 2) it reduces water flow velocity and inundation water depth, 3) it provides a life saving means by catching persons carried off by Tsunami, and 4) the mangrove can collects wind blown sands and raises dunes, which act as a natural barrier against Tsunami.

In order to use a coastal control forests more effectively as countermeasures against Tsunamis, it is important to evaluate the hydrodynamic effect of Tsunami control forest, and to further discuss a disaster prevention function. Tsunami numerical simulation model is used for explaining the degree of effective that are needed to consider the characteristic of mangrove forest. Harada and Imamura (2000) modeled the resistance force as drag and inertia forces based on Morison's equation. From the Tsunami numerical simulation models, the trunk volume of mangrove forest under water (V_o) and the basal area under water (A_o) are required to be solved accurately. Tree trunk diameter and stand density must be extracted.

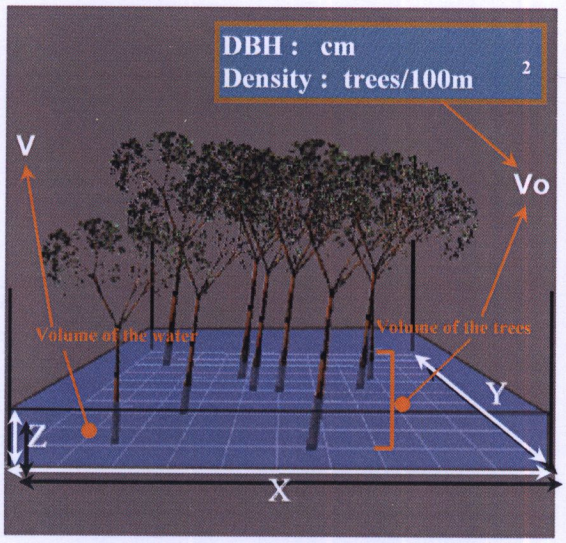

Figure 2.1 The model simulation of tree volume under the water (Wataru Ohira, JWRC)

2.1.2 Tsunami Simulation model

Explanation of the Tsunami simulation model is important to finally evaluate the impacts of Tsunami to coastal areas. Existence of forest in inundation areas surely reduces the impacts or damages of Tsunami. However, quantitative evaluation of this effect is required for understanding of the effects, planning of land use, conservation or creation of forest or green-belt. Thus, taking of an existence of forest into account in the simulation is very important. Accurate estimation of the effect is expected for proper understanding of the contribution of forest on Tsunami disaster mitigation. Usually, Tsunami propagation model is used for simulating the behavior of the wave from an epicenter to coast lines. Then, the process of run-up Tsunami propagation simulation programs is actually available. However, researchers do not consider the influence of forest to run-up process. More over, available programs are using leap-flog simulation scheme to solve shallow-water equation. Leap-frog scheme in run-up process is not stable because the process is associated with a shock-wave, thus there are a lot of approximation in calculation. This program will greatly contribute to the scientific quantitative estimation on forest's effect on reducing Tsunami damage at inundation area, planning conservation and creating of forest along coast lines, evacuation plan, and then finally to the well-being of the people who are living along coast lines.

2.2.3 Resistance of coastal forest in numerical simulation

In the numerical simulation, the effect of coastal forest is included as the resistance force in momentum equation. Harada and Imamura (2000) modeled the resistance force as drag and inertia forces based on Morison's equation and obtained the resistance coefficients of coastal forest against Tsunami by using the results of hydraulic experiment. Equations (1) are the resistance coefficients used by them, where C_D is the drag coefficient; Vo is the volume of tree under water surface in a constant volume; V is the volume of water in a constant volume; C_M is the inertia coefficient. The relation between the inundation depth and the vertical structure of trunk and leaf is varied this drag coefficient. These resistance coefficients include the effect of tree structure. In the numerical simulation, these resistance coefficients are used to calculate the forest effect quantitatively.

Resistance from Forest (Harada and Imamura, 2000)

$$C_D = 8.4\frac{V_O}{V} + 0.66$$

$$(0.01 < \frac{V_O}{V} < 0.07)$$

$$C_M = 1.7$$

$$f_x = \frac{C_D}{2}\frac{A_O}{\Delta x \cdot \Delta y}\frac{M\sqrt{M^2+N^2}}{D^2} + C_M\frac{V_O}{V}\frac{\partial M}{\partial t}$$

$$f_y = \frac{C_D}{2}\frac{A_O}{\Delta x \cdot \Delta y}\frac{N\sqrt{M^2+N^2}}{D^2} + C_M\frac{V_O}{V}\frac{\partial N}{\partial t}$$

$$A_0 = A_1 + A_2^{'}$$

$$V_0 = V_1 + V_2^{'}$$

$$A_1 = h_D \cdot dbh(\frac{N}{100}\Delta x \Delta y)$$

$$V_1 = h_D \pi \frac{dbh^2}{4}(\frac{N}{100}\Delta x \Delta y)$$

$$A_2^{'} = A_2(1-S_V)^{\frac{2}{3}}$$

$$V_2^{'} = V_2(1-S_V)$$

Tree shape and parameters

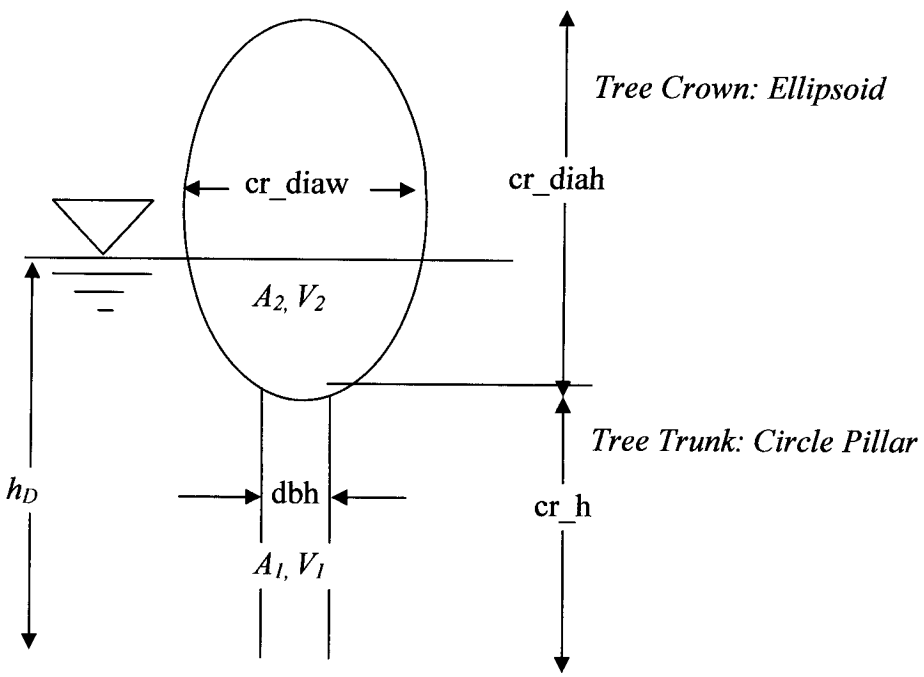

Figure 2.2 Tree shapes and parameter model

A_1 : Contribution of tree trunk to A_0

$A_2^{'}$: Contribution of tree crown to A_0

V_1 : Contribution of tree trunk to V_0

$V_2^{'}$: Contributikon of tree crown to V_0

h_D : Water Depth ($0 < h_D < cr\_h + cr\_diah$)

N : Number of tree stand in $100m^2$

cr_h : Bottom height of Tree crown

cr_diah : Size of tree crown (height)

cr_diaw : Size of tree crown (width)

dbh : diameter of tree trunk

A_2 : Projected area of tree cown to a direction under water in a control volume

V_2 : Volume occupied by tree crowns under water in a control volume

Tree crown is assumed to be an ellipsoid with cr_diah and cr_diaw

S_V : porosity of tree crown

The figure 2.3 shows that coastal forests have many functions to reduce Tsunami disaster as well as to decrease Tsunami energy. Table 1 shows the relationship between the functions and the effects of coastal control forest. The countermeasures that fully utilize the useful disaster prevention functions by these coastal natures should be taken into account. In order to extend or maintain the coastal forest as Tsunami prevention countermeasure, it is required to know the system of these functions in the coastal forest and to evaluate its effect by the simulation or field study on target area.

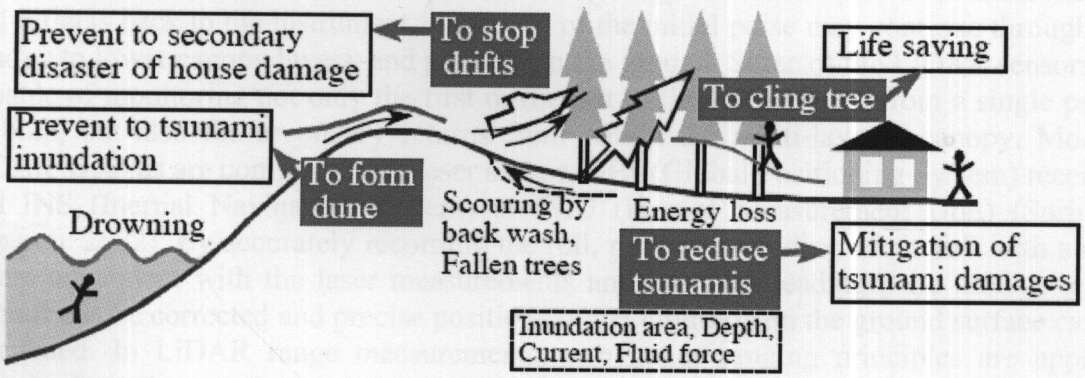

Figure 2.3 Functions and effects of coastal control forest to prevent Tsunami disaster Harada and Imamura (2000)

Table 2.1 Functions and effects of coastal control forest on Tsunami prevention Harada and Imamura (2000)

Functions of forest	Contents of functions	Effects of Tsunami prevention
Stop drifts	1. Stop drifts by forests 2. Prevent to crush drifts with house 3. Mitigate to house damage by drifts	Reduction of house damage
Resist to Tsunami	1. Trees resist Tsunami 2. Reduce Tsunami energy 3. Reduce inundation area and flow current	Reduction of inundation depth and current
Form dune	1. Collect wind blown sand and form dune 2. Act as natural barrier 3. Reduce Tsunami inflow	Reduction of inundation Tsunami
Cling tree	1. Parson cling tree 2. Prevent to wash away by Tsunami 3. Prevent the drowning death	Life saving

2.2 LiDAR Profiler

2.2.1 Background

LiDAR is the optical equivalent of radar and uses laser energy to measure the distance to a target and to accurately depict the earth surface in a three-dimensional format. An airborne LiDAR sensor sends laser pulses to the earth's surface and measures the range distance associated with the time difference between pulse generation and pulse return. When the sensor is flown over the forest canopy, the laser energy interacts with leaves and branches and reflects back to the instrument. A portion of the initial pulse may continue through the canopy to lower canopy layers, and possibly to the ground. Some of the LiDAR sensors are capable of monitoring not only the first or the last of the laser returns from a single pulse, or both, but also the secondary returns from within the multi-layered canopy. Modern LiDAR systems are composed of a laser sensor, GPS (Global Positioning System) receiver, and INS (Inertial Navigation System) or IMU (Inertial Measurement Unit) (Sorin C. Popescu. 2002). By accurately recording the roll, pitch and heading of aircraft with a time stamp coincident with the laser measurements and the GPS readings, the motion of the aircraft can be corrected and precise positions of the laser hits on the ground surface can be calculated. In LiDAR range measurements, two major ranging principles are applied, namely the pulse ranging and the phase difference. The latter is applied with lasers that continuously emit light. These lasers are called continuous wave (CW) lasers. In current ranging laser systems, mostly pulsed lasers are used (Sorin C. Popescu. 2002).

2.2.2 The Advantages of LiDAR data

LiDAR data is the useful information applied in the several fields. The following is a list of the main advantages of LiDAR (Chanchai, Phisan, 2004).

1. The data are all collected numerically.
2. The laser is an active sensor so it does not require specific sunlight conditions or even daylight. It can be flown under the clouds so well suited to tropical environment.

3. It is an aerial survey, so data are collected quickly and accurately and do not need field intervention.
4. The automated processing helps speed data analysis.
5. The high precision of the data allows its use for planning and detailed engineering it provides data in areas difficult to access or where it is environmentally sensitive.
6. And because the data are generic by nature (digital) they can be used in many different software packages and used to generate different views.

2.2.3 LiDAR versus photogrammetry

The principal overlap between LiDAR and photogrammetry lies in the 3-D measurement of surfaces. Baltsavias (1999a) presented a comparison between LiDAR and photogrammetry with a short overview of the major differences, advantages and disadvantages of each, and major applications. LiDAR affords the ability to "see" the ground in three dimensions. Even with a very dense canopy cover, there are often small openings in the canopy, because of the high sampling intensity. The laser beam will manage to reach the ground and produce a return. In contrast, photogrammetric methods, particularly automated cross-correlation techniques using infrared photographs, are often unable to accurately compute parallax in these small gaps due to substantially reduced illumination. As a result, the photogrammetric can often obtain elevations only at the top of dense canopies. Though LiDAR can have low penetration rates through a dense forest canopy, it offers a direct measurement of the ground elevation beneath the tree crowns.

In short, LiDAR has some strengths over photogrammetry, such as an increased density of points with known ground elevation beneath forest vegetation under certain conditions, independence of illumination conditions, mapping of surfaces 5 with poor texture and definition (ice, sand in coastal areas), fast response applications (e.g., natural disasters), direct acquisition of 3-D coordinates, and, as some studies suggest (Gomes Pereira and Wicherson, 1999, Petzold et al., 1999), The use of remote sensing techniques for assessing forest biomass has been investigated by other researchers, but as of yet such approaches have met with little success for multiage, multi-species forests, and only with limited success in forests with few species and age classes (Wu and Strahler, 1994). LiDAR has shown success in several forest types with large-footprint LiDAR, but applications of small footprint LiDAR to forestry have not progressed as far (Means, 2000).

2.2.4 Airborne lasers for vegetation assessment

The foundations of LiDAR forest measurements lie with the photogrammetric techniques developed to assess tree height, volume, and biomass. Aerial stand volume tables are based on estimation of two or three photographic characteristics of the dominant or co-dominant crown canopy; average stand height, average crown diameter, and percent of crown closure (Avery and Burkhart, 1994). The image spatial structure is only a two-dimensional representation of forest structure. In contrast, LiDAR pushes traditional remote sensing image processing for forest applications in the three-dimensional domain by being able to provide a unique metric, the vertical dimension of the canopy. LiDAR characteristics, such as high sampling intensity, ability to penetrate beneath the top layer of the canopy, precise geo-location, and accurate ranging measurements, make airborne laser systems useful for directly assessing vegetation characteristics. The first generation of LiDAR sensors used for remote sensing of vegetation was designed to measure the range to the first surface intercepted by the laser typically along singular transects defined by the flight line (Nelson *et al.*, 1988a, 1997, Ritchie *et al.*1993, Weltz *et al.*, 1994). More advanced laser altimeters, imaging or scanning LiDAR, are capable of scanning the ground surface beneath the

airborne platform, resulting in a true three-dimensional data set. Commonly, for such LiDAR sensors the laser beam sampling area, or footprint, is relatively small, usually less than 1m in diameter. An alternate type of laser altimeter, also known as surface LiDAR, utilizes the complete time-varying distribution of returned pulse energy, or waveform that results from the reflection of a single pulse with a large footprint (SorinC. Popescu, 2002).

2.2.5 Profiling LiDAR

LiDAR systems that sample along a single track defined by the flight line are known as single-transect or profiler LiDAR. The laser beam is pointed from the aircraft in a near nadir direction and normally operated in a repetitively pulsed mode. The resulting series of pulses can be used to derive the surface elevation profile. Bufton *et al.* (1991) provided the complete description of an airborne LiDAR system for profiling of surface topography that was able to measure laser pulse time-of- flight and the distortion of the pulse waveform for reflection from earth surface terrain features.

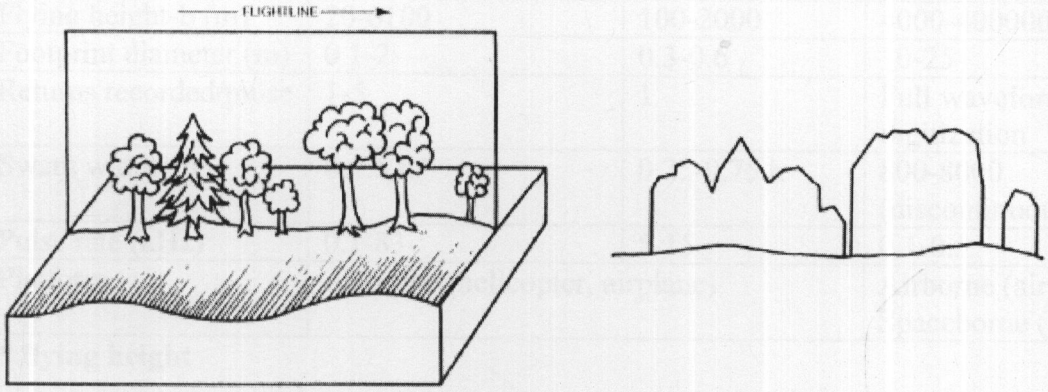

Figure 2.4 Canopy profile area observed with a profiling LiDAR (Nelson et al., 1984)

Single-track LiDAR was among the first system to demonstrate the potential of airborne laser data to measure quickly and quantitatively canopy structures and properties over large forest areas. The canopy profile area which is conceptualized in figure 2.3 and defined as the area between a trace of the top of the forest canopy and the ground over a given distance (Nelson, 1994) was initially estimated with photogrammetric methods (Maclean and Martin, 1984) and correlated with timber volume.

2.2.6 Scanning LiDAR

In early 1990s, profiling LiDAR sensors were gradually replaced by scanners, while GPS was combined with Inertial Navigation Systems (INS) or Inertial Measurement Unit (IMU). Airborne laser scanning represents a new and independent technology for the highly automated generation of digital terrain model (DTM) and digital surface model (DSM). Laser scanning systems provide overall vertical accuracy in the order of tenths of a meter, by operating usually at flying heights of up to about 1000m above ground. The scan angle is generally less than ± 30°, in most cases ± 20°. Present measuring rates, e.g. pulse repetition frequencies, situate between 2 kHz and 25 kHz. The actual sampling density is a function of flying speed, pulse rate, scan angle, and flying height. A given flying height above ground (H), the laser footprint (LF) mainly depending on the divergence of the laser beam g (rad) and the instantaneous scan angle (deg) are given by (Wehr and Lohr, 1999, Baltsavias, 1999b).

The high measuring rate of laser scanning is an important characteristic in airborne laser scanning. The ground point density is strongly dependent on the type of scanning system and the speed of the aircraft. The area samples not only rely on the laser ground footprint, but also on the point or post spacing across and along flight direction. A complete survey of existing commercial laser scanning systems and firms that include detailed systems parameters was provided by Baltsavias (1999c). Table 2.2 synthesizes different technical parameters of small and large footprint LiDAR that can be found in more detail in Dubayah et al., 1997, Baltasavias (1999c), Blair et al. (1999), and Means (2000).

Table 2.2 Comparative technical specifications of small and large footprint

Technical parameter	Small-footprint		Large-footprint (waveform return/pulse)
	Minimum-Maximum	Typical Values	
Point spacing (m)	0.1-10	0.3-2	10-25
Flying height-b (m)	20-6100	100-2000	4000-400000
Footprint diameter (m)	0.1-2	0.3-0.6	10-25
Returns recorded/pulse	1-5	1	Full waveform digitization
Swath width, m	0-1.5 h*	0.25-0.75 h	800-8000 (discontinuous)
Pulse rate (kHz)	0.1-83	5-15	0.1-0.5
Platform	Airborne (helicopter, airplane)		Airborne (airplane); Spaceborne (satellite)

*** flying height**

2.2.7 Scanning LiDAR applications in forest inventory

Previous investigations of using various configurations of LiDAR for forest assessment have returned positive conclusions regarding the estimation of tree heights, stand volume and biomass, and canopy cover. Most of the commercial laser scanners use a small footprint laser beam. Non-commercial and research systems mainly use large- footprint scanning laser systems, such as SLICER (Scanning LiDAR Imager of Canopies by Echo Recovery) and LVIS (Laser Vegetation Imaging Sensor) developed by NASA and used for validation of future space-borne LiDAR missions. Since the LiDAR data set used in this study was acquired with a small- footprint laser sensor, this review will concentrate more on this type of system and their applications in estimating forest parameters.

2.2.8 Mapping terrain topography with scanning LiDAR

The basic processing task that needs to be accomplished before attempting to estimate forest parameters is the characterization of the terrain elevation and creation of a DEM defined as a subset of the digital surface model obtained from raw laser points. Small footprint LiDAR is readily used to create high resolution DEM, 1x1m to 3x3m (Means, 2000), and characterize vegetation characteristics of relatively small areas. One of the major advantages that LiDAR offers over traditional photogrammetry is the ability to directly measure ground elevation in forested areas. Some of the laser pulses find openings in the canopy and penetrate to the ground or to lower layers of vegetation. These irregularly dispersed laser points assumed to correspond to the ground are used with appropriate interpolation methods to derive the high-accuracy DEM. Lam (1983) offered a comprehensive review of spatial interpolation methods classified as point and 16 aerial interpolation techniques. For point interpolation, the numerous methods can be further

classified into exact and approximate depending on whether they preserve the original sample point values. Exact methods include distance-weighting, Kriging, spline, polynomials and finite-difference methods. Approximate methods consist of power-series trend models, fourier models, distance-weighted least squares, and least-squares fitting with spline. Previous attempted to characterize the terrain elevation with LiDAR preferred to use exact interpolation methods in order to preserve the raw LiDAR data values (e.g. Young et al. 2000).

2.2.9 Deriving forest biophysical parameters with scanning LiDAR

• Vegetation height:

With a VCL signal, the first return above a threshold represents the top of the canopy, and the midpoint of the last return represents the ground return (Figure 2.5).

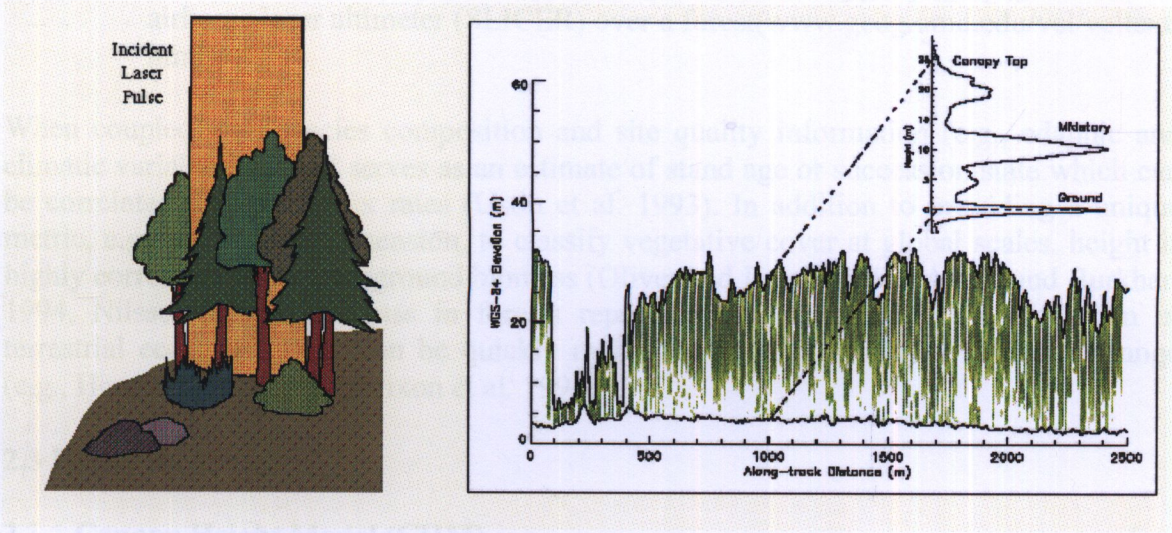

Figure2.5 Return waveform for a laser pulse (www.geog.umd.edu/vcl/vcltext.html)

An incident Gaussian laser pulse's interaction with surface structural components leads to the distorted (relative to a Gaussian) return waveform or echo (Ralph Dubayah et al. 2003). Measuring the return travel time of pulse gives distance from the sensor. By knowing where the last return is from the ground, shown as the strong pulse, this distance can be translated into height above the ground. The magnitude at any height of the waveform is directly related to the number of intercepting surfaces and their reflectance. Thus where the amplitude of the waveform is larger implies more canopy materials. The individual waveform contains multiple distinct returns, the independence of canopy top and ground topography, as well as the ability to detect the ground below the canopy. Figure 2 shows typical laser returns over a vegetation canopy. Canopy height is calculated by subtracting the elevations of the first and last returns. Vegetation height is a function of species composition, climate and site quality, and can be used for land cover classification alone or in conjunction with vegetation indices (e.g., NDVI). Along track measurements, i.e., footprint-to-footprint, of VCL-derived height variation provided additional information such as fractal (Palmer 1988) or auto-correlative (Cohen et al. 1990) properties of the canopy that further may be used to differentiate among natural and anthropogenically-disturbed land cover patterns (Krummel et al. 1987).

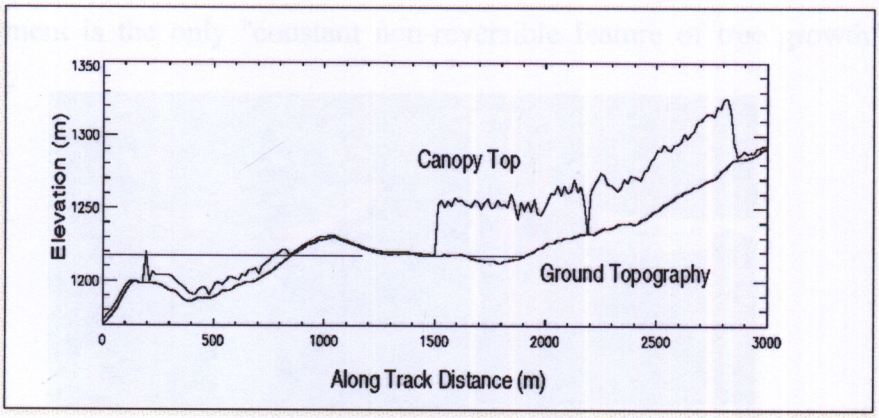

Figure 2.6 Profile of canopy height, canopy density and sub-canopy topography from an airborne laser altimeter (SLICER) over a forest(www.geog.umd.edu/vcl/vcltext.html)

When coupled with species composition and site quality information (e.g., edaphic and climatic variables), height serves as an estimate of stand age or succession state which can be correlated to carbon flux rates (Ustin et al. 1993). In addition to providing a unique metric, e.g., the vertical dimension, to classify vegetative cover at global scales, height is highly correlated with aboveground biomass (Oliver and Larson 1990; Avery and Burkhart 1994, Nilsson 1996). Biomass in forests represents the major reservoir of carbon in terrestrial ecosystems that can be quickly mobilized by disturbance or land use change (e.g., Houghton et al. 1987; Dixon et al. 1994).

2.3 Forest attributes

2.3.1 Canopy Height Model (CHM)

The tree canopy height model was computed as the difference between tree canopy hits and the corresponding DEM values. Tree canopy hits or first-return LiDAR points are usually interpolated to a regular grid that corresponds to the digital surface model.

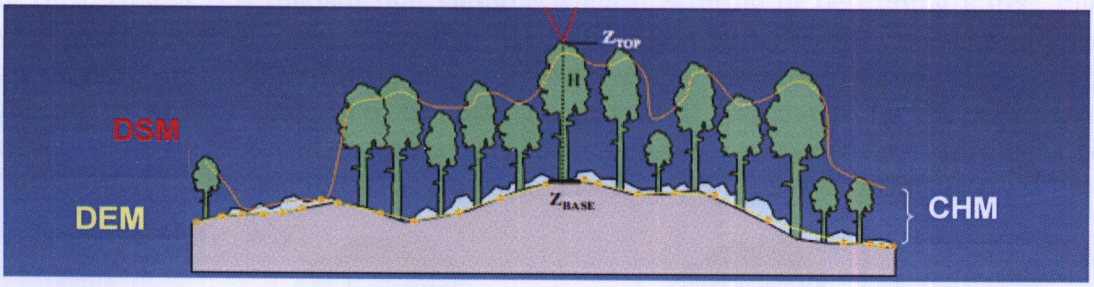

Figure 2.7 The canopy height model

2.3.2 DBH

DBH stands for diameter at breast height. DBH is a standard method of expressing the diameter of the trunk of a tree and the outside bark diameter at breast height. It is an important factor in order to express the hydraulic resistance of Tsunami energy. The two most common instruments used to measure DBH are a girthing (or diameter) tape and calipers. The trunk is measured at the height of breast defined as 4.5 feet (1.37m) above the forest floor. Moreover, DBH is used to estimate the amount of timber volume in a single tree or stand of trees utilizing the correlation between stem diameter, tree height and timber volume (Mackie, 2006). It can also be used in the estimation of the age of trees given that

diameter increment is the only "constant non-reversible feature of tree growth" (White, 1998).

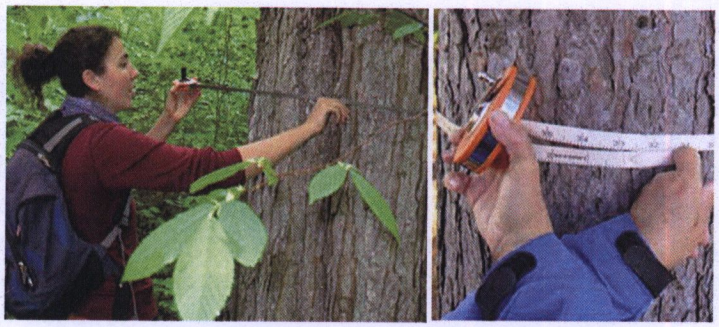

Figure 2.8 Measurement of DBH using the diameter tape (www.nrri.umn.edu)

2.3.3 Tree crown diameter

For particularly conifers occurring in open-grown and even-aged stands, crown diameter is closely correlated with stem DBH. For example, Leech (1984) established that crown width for open-grown Radiata pine in South Australia was linearly related to tree DBH. This relationship was independent of site quality. For 109 observations, the weighted estimate of the relationship was:

$$CW = 0.7544 + 0.2073*d$$

where: CW is crown width (m) and d is DBH (cm)

Leech's model can be used as the base for an index of stand density called Crown Competition Factor (CCF) which his suggestion may be useful in studies of the growth and yield of Radiata pine because the CCF is independent of age and site. Because of the strong correlation between crown diameter and DBH, tree volume tables based on crown diameter can be compiled for use with aerial photographs.

2.3.4 Tree height

Total height is defined as the vertical distance from the base of the tree to the uppermost point (tip). Height is a fundamental variable when measuring or describing a tree. Plants may not be defined as trees unless they have the potential to reach a minimum defined height (e.g. Specht 1970 defined a tree as a woody plant more than 5 m tall, usually with a single stem), while forests may be distinguished from woodlands by the number and potential or actual height of the trees (e.g. Specht defined woodlands and forests as both having trees, but with the projective crown cover of forests greater than 30%).

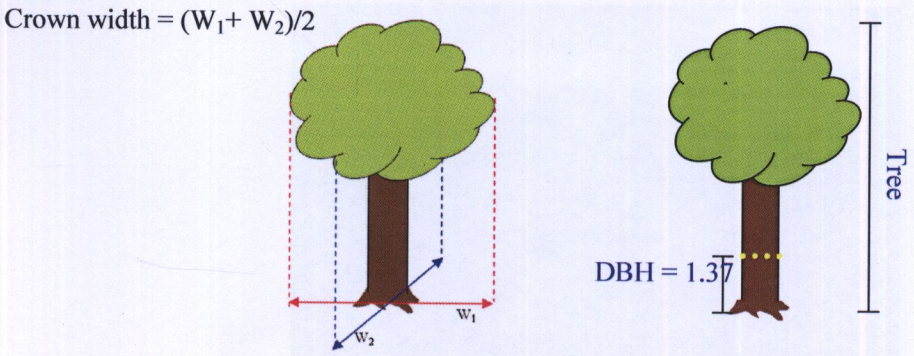

Figure2.9 The crown width, tree height and DBH measuring

2.3.5 Stem volume

In managing a forest for commercial timber production, an estimation of the stem volume of wood is essential. Such estimation is also important for determining biomass of the forest, the amount of carbon storage, fuel sources etc. The estimation is based on the volume of individual tree both directly or indirectly. Despite the fact that each year, more and more wood is being sold by weight, the forest manager still uses volume data extensively whether they are derived from inventories or yield tables/functions. Even though sale, processing and marketing procedures are changing, volume and the measures used to derive them (diameter, height, form, stand basal area, top height, etc.), are still most important tree and stand parameters. The unit of measurement may be cubic meters or cubic meters per hectare.

2.3.6 Relationship of forest parameter

There is a close relationship between tree parameters: diameter, height, crown size and bole volume (Philip, 1994). Using these algometric relationships, a dimension of measurement can be easily estimated by means of other dimensions (Mahmut D. Avsar 2004). As a mater of fact using the height-DBH relationship, height can be estimated by means of DBH. In the study of M.D. Avsar (2004), there were strong relationships between three variables: DBH, crown diameter and height of Calabrian pines. The strongest relationship is the height-DBH relationship (R^2=0.82) followed by the crown diameter-DBH (R^2=0.74) and crown diameter-height (R^2=0.62). The study indicated that height-DBH relationship can be described by the second-degree polynomial model, while the crown diameter-DBH and crown diameter-height relationship can be explained by the power model. In contrast, Hasenauer (1997) determined that the relationship between crown diameter and height was generally strong in various tree species and this relationship could be described by the simple linear model.

2.4 Mangrove forest in Thailand

Mangrove generally is tree and shrub that grows in saline coastal habitats in the tropical and sub-tropical tidal areas. A mangrove forest thrives along the coastline within the estuaries of rivers where alluvium brought down by the rivers is deposited. They are able to survive inundation by salt water and in soil which is unstable. The degree and frequency of inundation largely determine species distribution. Areas where mangroves grow include estuaries and marine shorelines with spared to physical conditions. They also have to deal with swollen rivers carrying silt during the wet season, as well as violent storms that hit the coasts.

Figure 2.10 The generality mangrove forest in Thailand (www.talaythai.com)

Distributions of mangrove in Thailand show in the figure 2.12 referred from Department of marine and coastal resources, 2004.

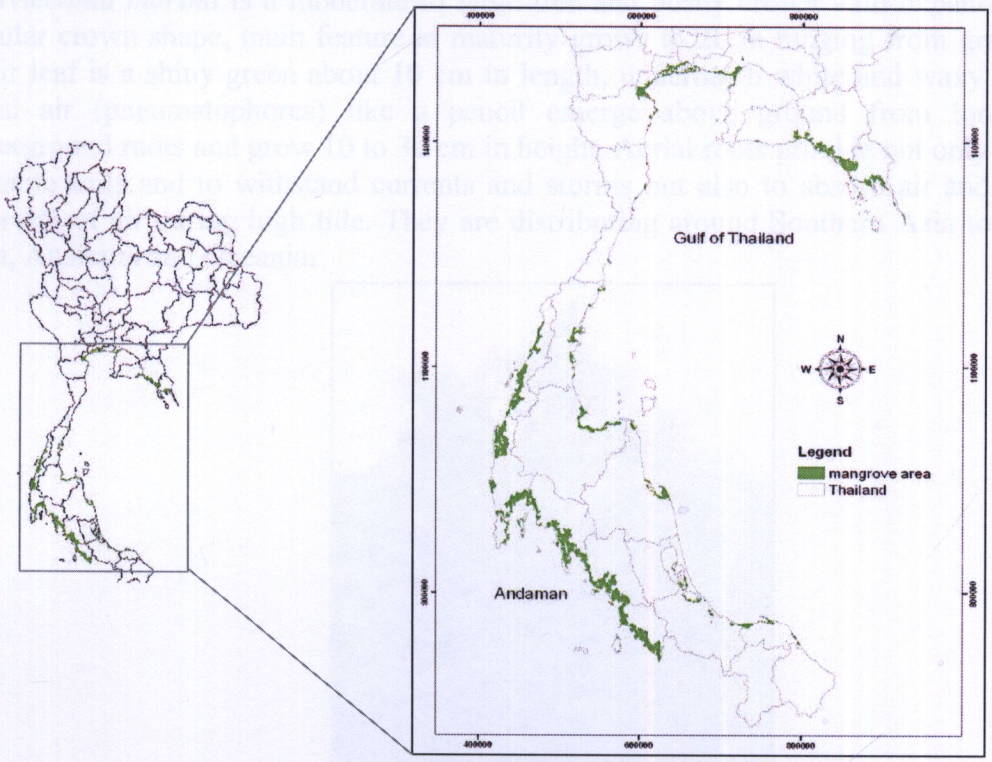

Figure 2.11 Distributions of mangrove forest in Thailand

The community of mangrove forest composite of the many species that can classify to three community group.

1) Pioneer species community such as *Avicennia alba* (Sa Mae Kao) and as *Avicennia marina* (Sa Mae Taray).
2) Rhizophora species community such as *Rhizophora mucronata* (Kong Kang Bai Yai) and *Rhizophora apiculata* (Kong Kang Bai Lek). Rhizophora usually have a prop root that are useful for carry the tree from wave and protect the shoreline.
3) Mixed species community such as *Ceriops decandar, Ceriops tagal, Bruguiera sexangula, Bruguiera gymnorrhiza* and *Nipa fruticans etc.*

1) 2) 3)

Figure 2.12 The examples of mangrove species in each community 1) *Avicennia marina* 2) *Rhizophora apiculata* 3) *Ceriops tagal*

2.5 The characteristics of *Avicennia marina* (Sa Mae Taray)

In this research, *Avicennia marina* (Sa Mae Taray) is concentrated. General characteristics of *Avicennia marina* is a moderate to large tree and bushy crown with expanded, almost circular crown shape, main feature at maturity grows to 20 m ranging from gray to dark. Their leaf is a shiny green about 10 cm in length, underneath white and waxy. Roots are aerial air (pneumatophores) like a pencil emerge above ground from long shallow underground roots and grow 10 to 30 cm in height. Aerial roots provide not only support in unstable soils and to withstand currents and storms but also to absorb air and provide a reservoir of air during high tide. They are distributing around Southern Asia to Southeast Asia, Australia and Oceania.

Figure 2.13 *Avicennia marina* or Sa Mae Talay tree take at the Bang Poo

Science name: *Avicennia marina*
Family: AVICENNIACEAE
Local name: Sa Mae Taray (Thailand)

Table 2.3 Table The characteristic of *Avicennia marina*

Function	**General characteristics**
DBH	5 – 30 cm.
Height	8 -20 m.
Crown width	3 to 16 m.
Crown shape	usually egg-shaped, elliptic or lance-shaped
Leave	light green about 10 cm long
Growth rate	Rapidly

CHAPTER III

METHODOLOGY

The methodology separate to two scenarios base on the objective. This sub-chapter describes the research beginning with the scenarios one (figure3.1) that is the extraction of tree canopy height model through the raw LiDAR point data. In parallel, field observation which consists of tree height, crown width and DBH must be done. The IDL free code namely TreeVaW plays the important role to extract tree height, crown width from CHM. With the derived- LiDAR tree height, crown width and DBH, the relationship of those were investigated in single tree crown level. The DBH algometric model is set up to estimate the DBH from LiDAR. The model validation is performed in the final step. Second scenario of this study is the calculation of the trees volume (Vo) and projected area Ao under water for Tsunami Run-up Model. The stem volume equation of mangrove tree that is a function of DBH and tree height used to develop the trunk diameter function. The overall methodologies can be summarized in the figure 3.2 the details for each step are deeply explained below.

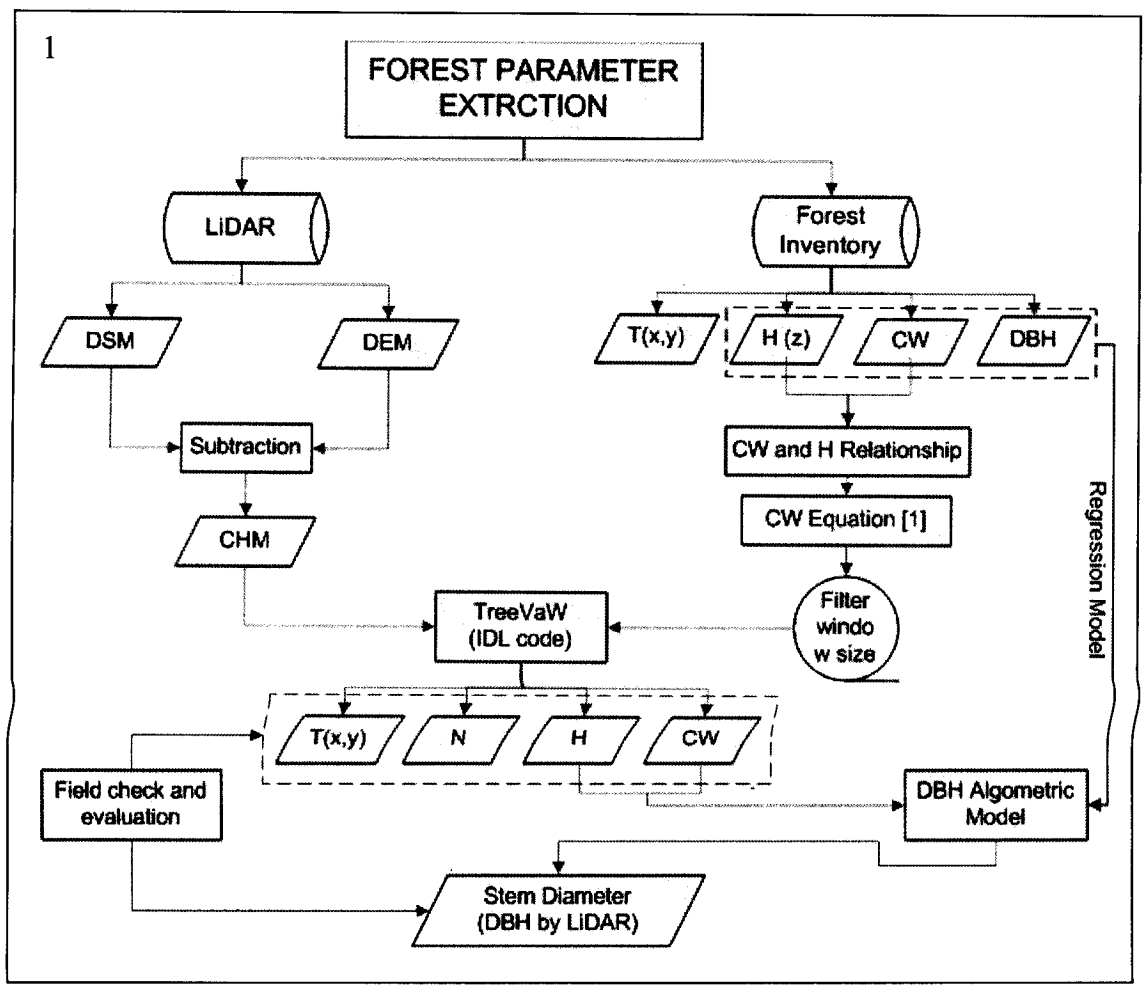

Figure 3.1 Flowchart of scenario one.

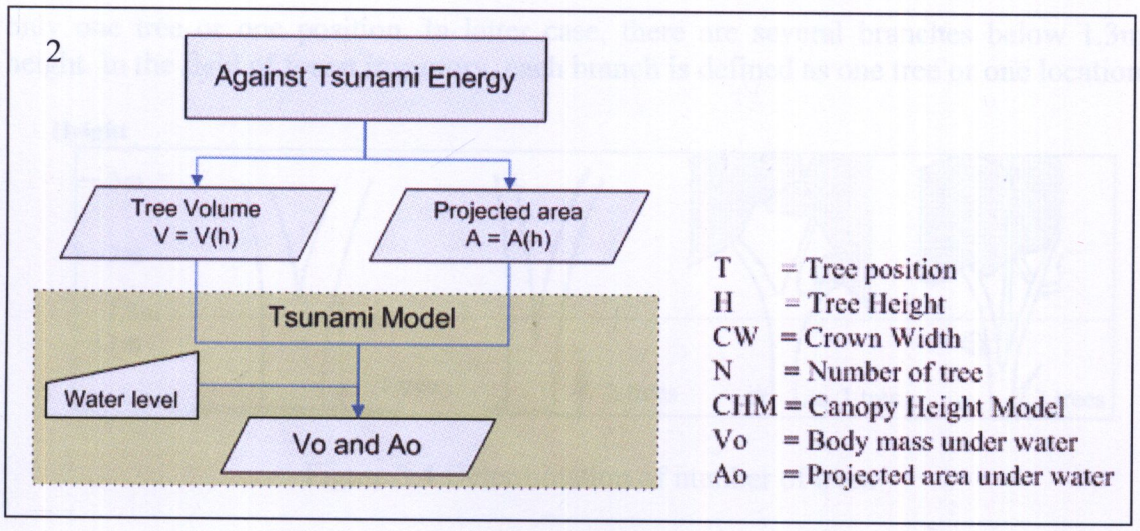

Figure 3.2 Flowchart of scenario one.

3.1 Data collection

The in situ data were collected during December 2008 - February 2009 by measuring the tree attributes in 100m x 120m of plot. An individual tree measurement was taken for their position, height, crown width and DBH. Sampling trees with diameter at breast height (1.3m) were measured in following processes:

• Study plot implementation

Temporary plot with the size of 100m x 120m illustrated in figure 3.3 was determined to derive mangrove parameters. Initially, referent point was defined at lower left corner. This point position was measured by GPS. Remaining corners were marked by using compass and tape for angle and distance measurement respectively. Lower right corner was plotted in south direction (180°) along the coastal line. In vertical, upper left and right corners was marked in east direction (90°). Subsequently, sub- quadrant with interval 10m were set up both in vertical and horizontal sides resulting in 10m x 10m window size.

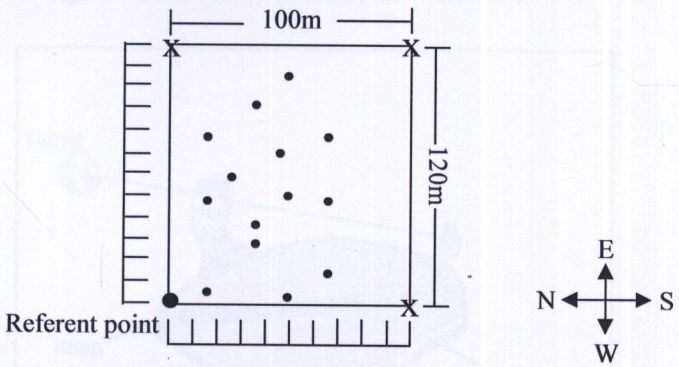

Figure 3.3 Plot implementation in study site

• Measurement of individual tree position

The positions of tree in the plot were determined by the distance from referent point which has the exact position by GPS in UTM WGS84 coordinate. The distance was measured in horizontal for Northing position (Y) and in vertical for Easting position (X). With the complicated shape of mangrove tree, there are two main types: single main branch and multiple branches. In former case, there is one branch in 1.3m height range. So there is

only one tree or one position. In latter case, there are several branches below 1.3m in height. In the field of forest inventory, each branch is defined as one tree or one location.

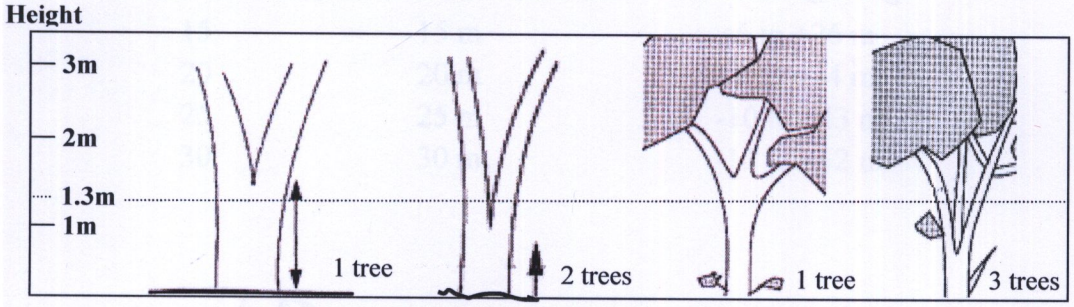

Figure 3.4 Determination of number of trees

• Tree height measurement

Manual height measurements were done for each tree location. To do so, forest inventory instrument, namely Haga altimeter was used for height measurement. Following below is the process to measure tree height.

(1) The "Haga" altimeter measures the angle of elevation and angle of depression directly for known horizontal distances (base length).
(2) The base lengths were determined by turning a knop options (15, 20, 25 or 30 m) depending on vision, crown size and measuring range.
(3) Measurement of the baseline distance from the tree to observed point
(4) Measurement of angle of elevation α_1 by pointing to the tree top and the ground bottom
(5) Height (h_1) was calculated by
$h_1 = \tan\alpha_1 \times$ baseline distance
(6) Measurement of angle of depression α_2 by pointing to the bole of tree and the ground bottom
(7) Height (h_1) was calculated by
$h_2 = \tan\alpha_2 \times$ baseline distance
(8) The total tree height can be calculated by $H = h_1 + h_2$.

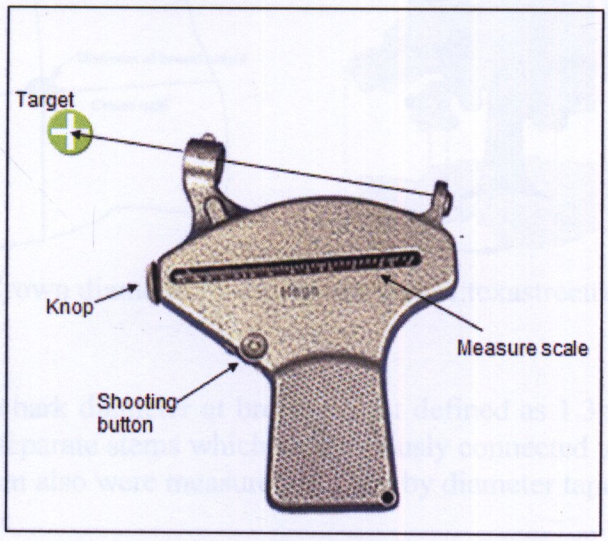

Figure 3.5 Haga Altimeter

Table 3.1 Ratio of required baseline distance

Scales	Required Baseline Distance	Measuring Range
15	15 m	-6 to +26 m
20	20 m	-8 to +34 m
25	25 m	-10 to +43 m
30	30 m	-12 to +52 m

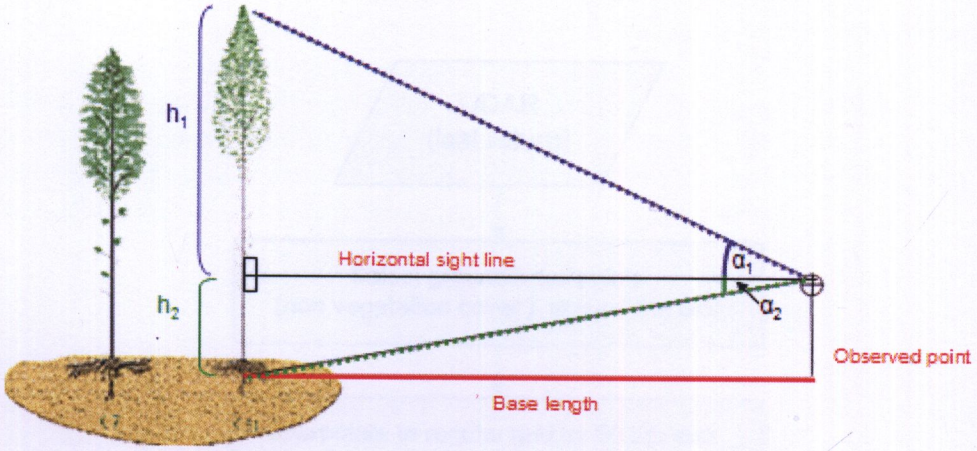

Figure 3.6 Process to measure tree height

• Measurement of crown diameter

Crown width which is the projecting edges of the crown to the ground was determined as an average of four perpendicular crown radius measured with a meter tape from the tree bole towards each cardinal direction as shown in figure 3.7.

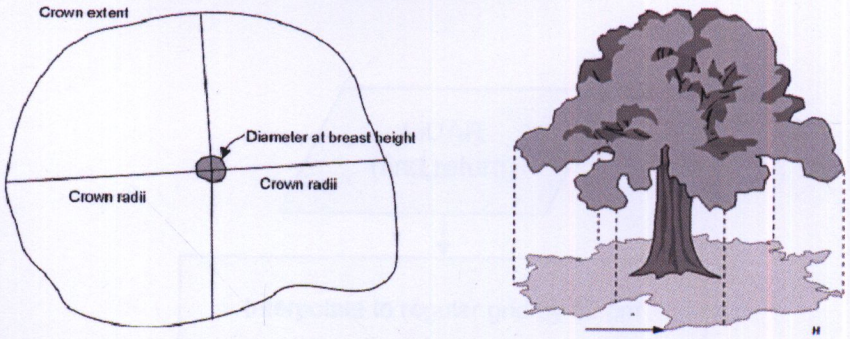

Figure 3.7 Crown diameter measurement (www.texastreetrails.org/)

• DBH Measurement

The DBH is the outside bark diameter at breast height defined as 1.3m above the ground. In multiple stem cases, separate stems which are obviously connected to one another below breast height so each stem also were measured at 1.3m by diameter tape.

3.2 Digital Elevation Model

Basic task before attempting to determine the tree height is the characterization of the ground elevation. DEM is defined as the representation of continuous elevation values over a topographic surface by a regular array of z-values. An iterative approach was used to construct the DEM from the raw LiDAR data point using only the last return elevation values. The first step of the algorithm for constructing the DEM is the selection the ground laser point (non vegetation area cover) around the study plot by assumption the ground is flat. The linear kriging technique was chosen for interpolating from dispersed LiDAR points to a regular grid only exploiting the selected laser point.

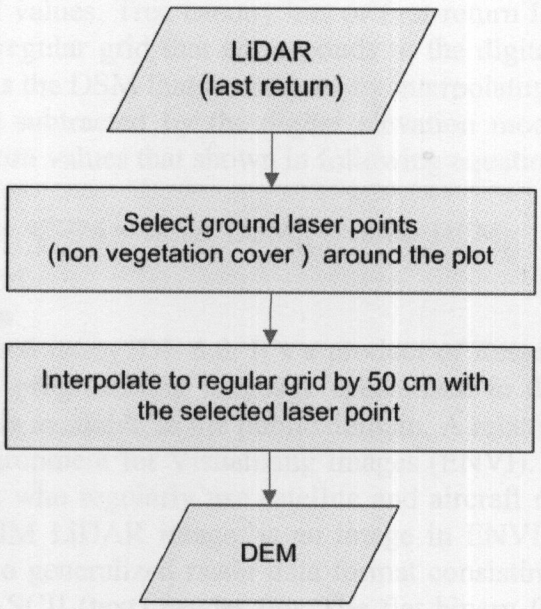

Figure 3.8 Flowchart of the algorithm for generating DEM

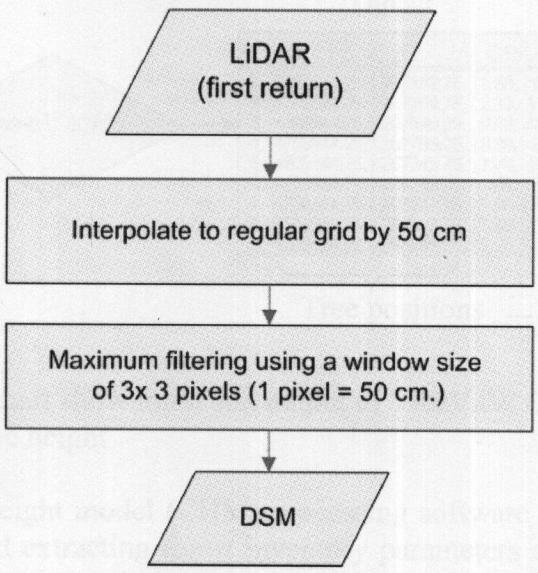

Figure 3.9 Flowchart of the algorithm for generating DSM.

3.3 Digital Surface Model

Digital surface model (DSM) is the topographic map of the earth's surface. The DSM data includes buildings, vegetation, and roads, as well as natural terrain features. DSM is calculated by taking the advantage of the first return (vegetation point) of raw LiDAR data point. With the LiDAR-derived DSM, the tree canopy was illustrated by a regular array of z-value. LiDAR point elevation was interpolated to be as a regular grid with a spatial resolution of 50 cm to get an accurate characterization of the top canopy surface.

3.4 Canopy Height Model (CHM)

Canopy Height Model or CHM is described as the difference between tree canopy hits and the corresponding DEM values. Tree canopy hits or first-return LiDAR points are usually interpolated to be as a regular grid that corresponds to the digital surface model (DSM). The tree canopy model is the DSM that is obtained by interpolating the first LiDAR returns to be as a regular grid subtracted by the digital elevation model (DEM) that takes an advantage of the last return values that shown in following equation.

$$CHM = value\_DSM_{ij} - value\_DEM_{ij}$$

3.5 TreeVaW algorithm

Treevaw was implemented using IDL 6.0. It's a product of Research Systems Inc., which is the fourth generation programming language specialized in data visualization. A free distribution of Treevaw is available in the public domain. A related product from Research Systems Inc. is the Environment for Visualizing Images (ENVI). It's an image processing system targeted at users who regularly use satellite and aircraft remote sensing data. The input to Treevaw, a CHM LiDAR image, is an image in ENVI format. When handling images, ENVI employs a generalized raster data format consisting of a simple flat binary file and an associated ASCII (text) header file. The flat binary file is made up of pixels, which corresponds to the CHM LiDAR points. Whereas, the ASCII header file contains important attributes such as the resolution of the pixels, the number of pixels, and the Universal Transverse Mercator (UTM) co-ordinates of the forest plot under consideration.

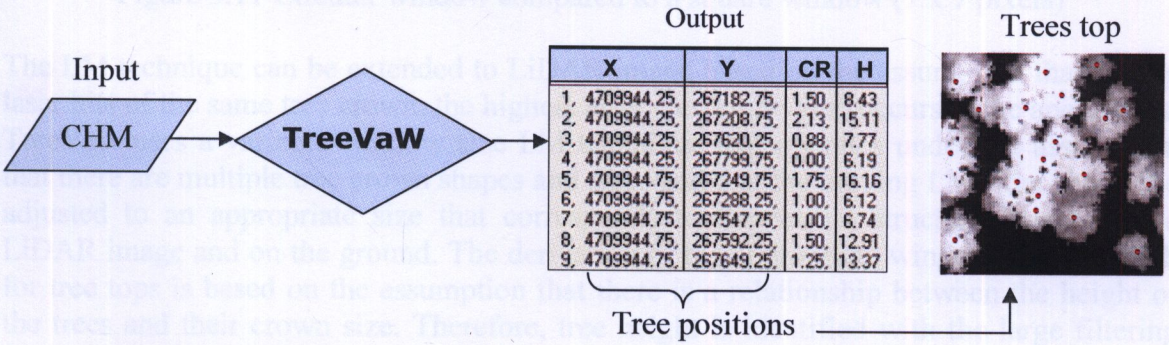

Figure 3.10 The chart show input and output of TreeVaW CR: Crown Radius, H:Tree height

TreeVaW is a canopy height model (CHM) processing software implemented in IDL and focusing on locating and extracting forest inventory parameters at an individual tree level from a LiDAR-derived canopy height model such as tree location, height and crown diameter. The input is a LIDAR-derived canopy height model (CHM) in ENVI image

format. TreeVaW can also be used with appropriate settings for processing multispectral imagery-derived CHM. The output consists of individual tree positions, tree height, crown radius and number of tree.

3.6 Extraction of mangrove forest parameter

3.6.1 Tree height and crown width extraction

This step is developed for the estimation of tree heights and crown width from CHM based on single tree identification using local maximum (LM) filtering with a variable window technique. Local maximum filtering is a common technique used to identify tree location using specified, moving window with 3x3 or 5x5 being the typical window size (Niemann et al., 1999; Pinz, 1999). The LM technique operates on the assumption that high laser values in a spatial neighborhood represent the tip of tree crown.

Successful identification of tree location using the LM technique depends on the careful selection of the filter window size. If the filter size is too small or too large, error will be occurring. Thus, the variable window LM technique functions under the supposition that there is multiple tree crown sizes and that the moving LM filter should be adjusted to be an appropriate size corresponding to the tree crown structure. Tree crown most closely can be projected within a circle. Therefore, it is evident that searching for the LM to identify individual crowns with a circular window of variable diameter is more appropriate than filtering with a square window.

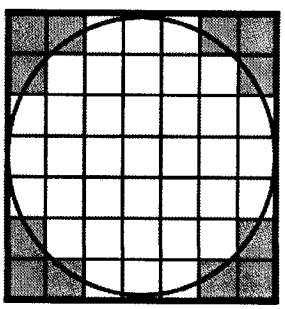

Figure 3.11 Circular window compared to a square window (7 x 7 pixels)

The LM technique can be extended to LiDAR image based on the assumption that among laser hits of the same tree crown, the highest laser elevation value occurs at the apex. Thus, TreeVaw uses a variable window size LM technique that operates under the assumption that there are multiple tree crown shapes and sizes and that the moving LM filter should be adjusted to an appropriate size that corresponds to the spatial structure found on the LiDAR image and on the ground. The derivation of the appropriate window size to search for tree tops is based on the assumption that there is a relationship between the height of the trees and their crown size. Therefore, tree height is identified with the large filtering window sizes, while short trees are identified with smaller filtering windows. The processing algorithm reads the heights and dynamically varies the window size to search for the local maximum based on biometrics relationships between tree height and crown size derived from field inventory data.

3.6.2 The relationship between tree height and crown width

The derivation of the appropriate window size to search for the tree tops is based on the assumption that there is a relationship between the height of trees and their crown size.

Crown size was considered as the dependent variable. The higher the trees, it should be the larger the crown size. Thus, tree height and crown size data from the field inventory were used to derive a relationship between tree height and crown size. Linear and nonlinear regression models were tested for mangrove tree; *Avicennia marina* by SPSS statistical software. Subsequently, the correlation equations of tree height and crown width were used to determine the circular window size for calculating crown width and to find the appropriation of the circular filtering window size for identifying the tree top.

$$Cw = f(h)$$

where: Cw = Crown width
H = Tree height

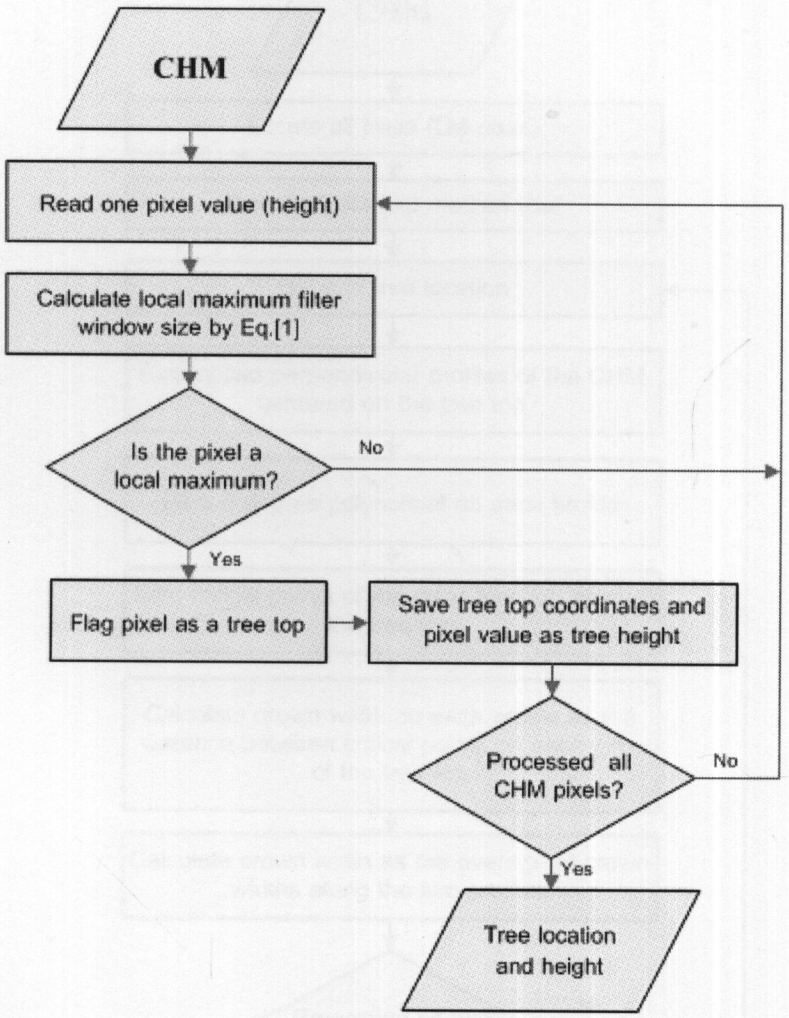

Figure 3.12 Flow chart of the algorithm for locating trees and measuring height by TreeVaW (Popescu, 2002)

3.6.3 Tree location and height measurement

The tree tops and tree height were identified by taking the advantages of TreeVaW algorithm implemented in IDL code. First step was the reading of the height value pixel by pixel on canopy height model (CHM) and calculation of the window size to search for the local maximum by using equation [1] that is based on the relationship between height and

crown size. If the current pixel corresponds to the local maximum, it is flagged as a tree top. The canopy 3-D surface of laser heights (CHM) was sampled only at the positions of the tree apex to find out the height of each tree. Then, tree top coordinates and pixel value were recorded all CHM pixels. The tree location, height and number of tree were the outputs in this section.

3.6.4 Crown diameter extraction

Crown width measurement was generating by TreeVaW algorithm. The algorithm for measuring crown diameter uses the tree locations identified with local maximum filtering form provides step.

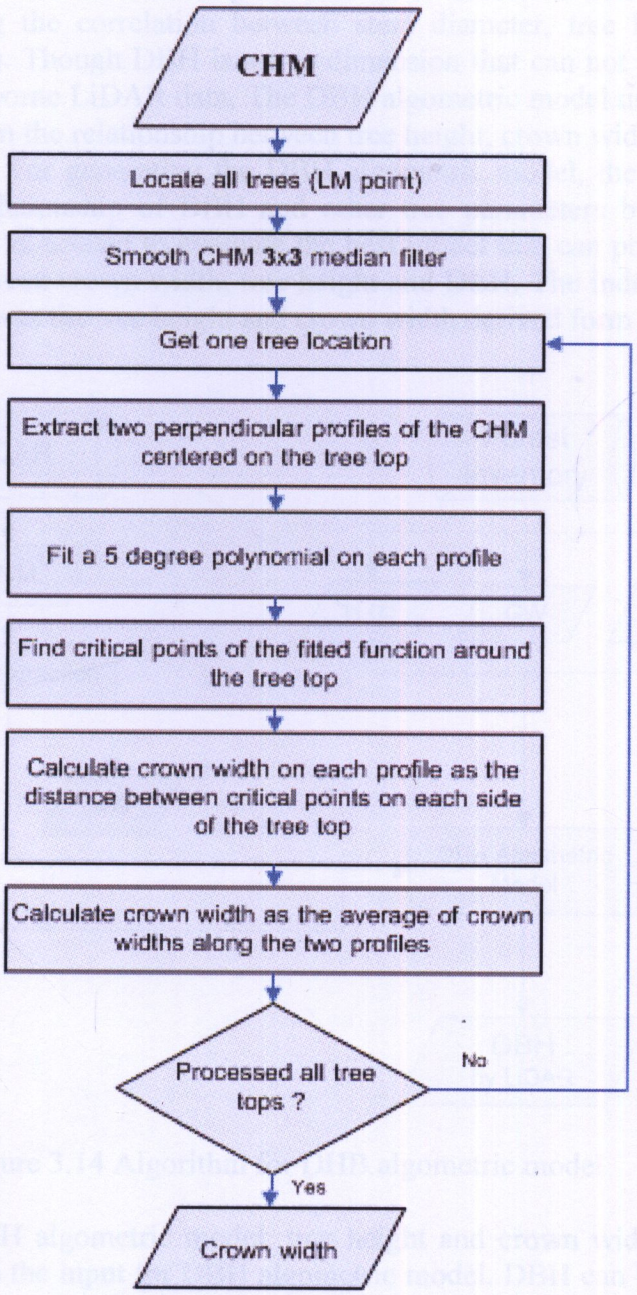

Figure 3.13 Flowchart of the algorithm for measuring crown width by TreeVaW (Popescu, 2002)

The details of crown diameter extraction see in Popescu 2003 and can be summarized as following: (1) Smooth 3 x 3 median filter on CHM dataset (2) get tree location (3) two perpendicular profiles of the CHM are extracted, centered on the identified tree top; (4) a 5-degree polynomial is fitted to each profile; (5) critical points of the fitted functions are identified; and (6) the crown diameter is calculated as the average distance between critical points on the two perpendicular profiles. The LiDAR-derived tree measurements were analyzed with the regression models and cross validation to estimate the field-measured crown diameter.

3.7 DBH algometric Model

Diameter at breast height, or DBH, is a standard method of expressing the diameter of the trunk of a tree. DBH is used in estimating the amount of timber volume in a single tree or stand of trees utilizing the correlation between stem diameter, tree height and timber volume (Mackie, 2006). Though DBH is a tree dimension that can not directly visible on CHM derived from airborne LiDAR data. The DBH algometric model used to estimate the DBH by LiDAR base on the relationship between tree height, crown width, and DBH from ground inventory data. For generating the DBH algometric model, the regression model used to explant the relationship of DBH and other tree parameters by SPSS statistical program. Several times is needed to evaluate the best model that can provide the strength of the relationship between crown width, tree height and DBH. The independent variables when estimating DBH was the tree height and crown width derived form LiDAR.

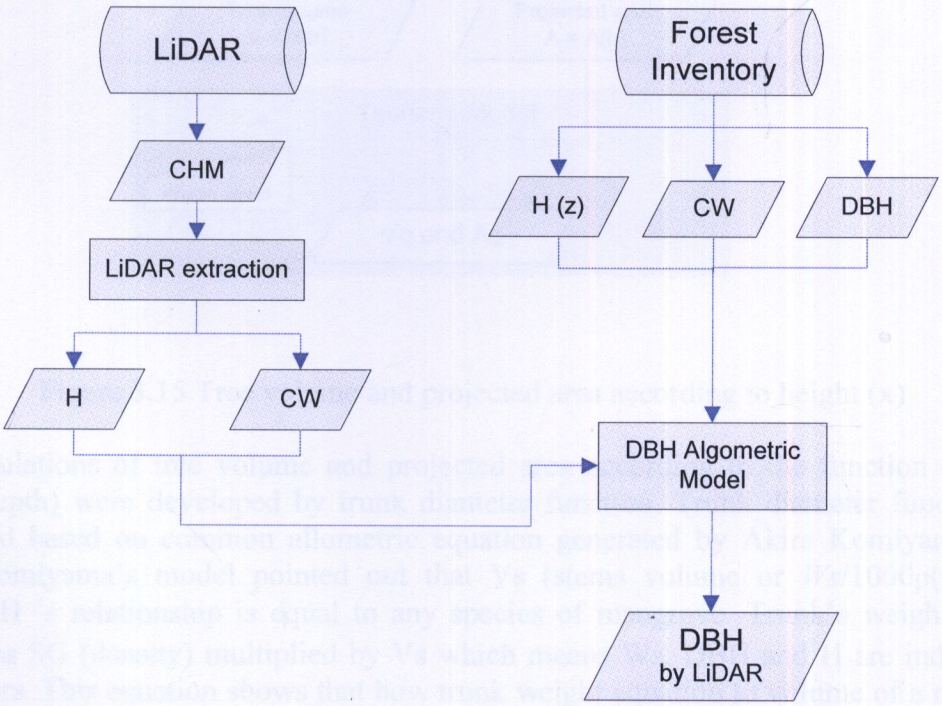

Figure 3.14 Algorithm for DHB algometric model

After receiving the DBH algometric model, tree height and crown width extracted from LiDAR were used to be the input for DBH algometric model. DBH can be estimated from the model when the crown width and tree height from LiDAR were available.

$$DBH = f(Cw, H)$$

DBH : Estimating of diameter at breast height
Cw : Crown width derived form LiDAR
H : Tree height derived form LiDAR

3.6.6 Model validation for tree attribute estimation

To evaluate the effectiveness of estimated function, estimated parameters were compared with inventory data e.g. tree location, tree height, crown width, number of tree and DBH. Afterward, the correlation coefficient and the RMS error were analyzed by below equation.

$$RMSE = \sqrt{\frac{\sum_{i=1}^{n}(X_{esti} - X_{ref})^2}{N}}$$

3.7 Estimation of effective stems volume and projected under water

Tree volume (V_o) and projected area (A_o) affecting to the resistant force against the Tsunami wave are the critical parameter for Tsunami run-up model under water.

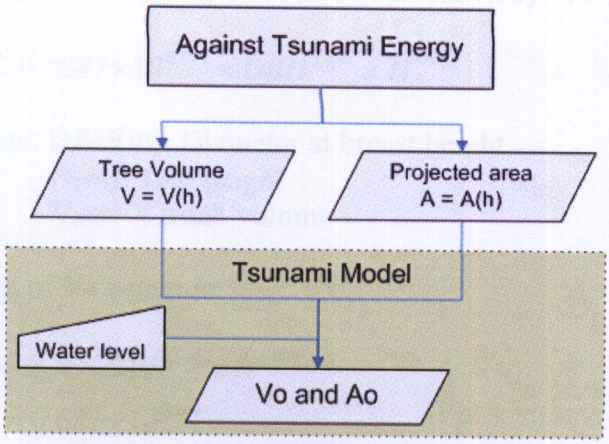

Figure 3.15 Tree volume and projected area according to height (x)

The calculations of tree volume and projected area according to the function of height (water depth) were developed by trunk diameter function. Trunk diameter function was developed based on common allometric equation generated by Akira Komiyama et al., 2005. Komiyama's model pointed out that Vs (stems volume or $Ws/1000\rho(m^3)$) and $DBH^2 \times H$ *'s relationship is equal to any species of* mangrove. Trunk's weight (Ws) is derived as SG (density) multiplied by Vs which means Ws, DBH and H are independent parameters. This equation shows that how trunk weight equation to volume of a mangrove tree can be transformed.

Komiyama's model

$$Ws = 0.0687\rho(DBH^2 \times H)^{0.931}$$

where: DBH(cm): Diameter at breast height
H(m): Tree height

Ws(m^3): Trunk volume
ρ(t/m^{-3}): Mean wood density of mangroves

Equation for transforming DBH in centimeter to meter

$$\overline{DBH} \times 100 = DBH$$

where: $\overline{DBH} : (m)$

$$\begin{aligned} Ws &= 0.0687\rho(10^4 \times \overline{DBH}^2 \times H)^{0.931} \\ &= 0.0687\rho \times 10^{3.724} \times \overline{DBH}^{1.862} \times H)^{0.931} \\ &= 0.0687\rho \times 10^{3.724} \times \overline{DBH}^{1.862} \times H^{0.931} \\ Vs &= \frac{Ws}{1000\rho} = 0.0687 \times 10^{0.724} \times \overline{DBH}^{1.826} \times H^{0.931} \end{aligned}$$

Thus, Trunk volume of a mangrove tree can be calculated by: Vs

$$Vs = 0.0687 \times 10^{0.724} \times DBH^{1.826} \times H^{0.931}$$

where: DBH(m): Diameter at breast height
H(m): Tree height
Vs(m^3): trunk volume

To identify constant of Vs equation

$$\begin{aligned} Vs &= \pi \cdot C \cdot DBH^{1.862} \times H^{0.931} \\ \pi C &= 0.687 \times 10^{0.724} \\ C &= \frac{0.0687 \times 10^{0.724}}{\pi} \\ C &= 0.115826215 \end{aligned}$$

To reckon the tree volume and projected area regarding function of tree height, trunk diameter function r(h) or R(x) were assumed to explain the attributes of tree trunk shape. Trunk diameter function uses the cylinder shape for generating the tree trunk shape radius from ground to DBH level ($h<1.3m$) and $y = ax^b$ for generate the tree trunk shape radius from DBH level to tree top ($h > 1.3m$).

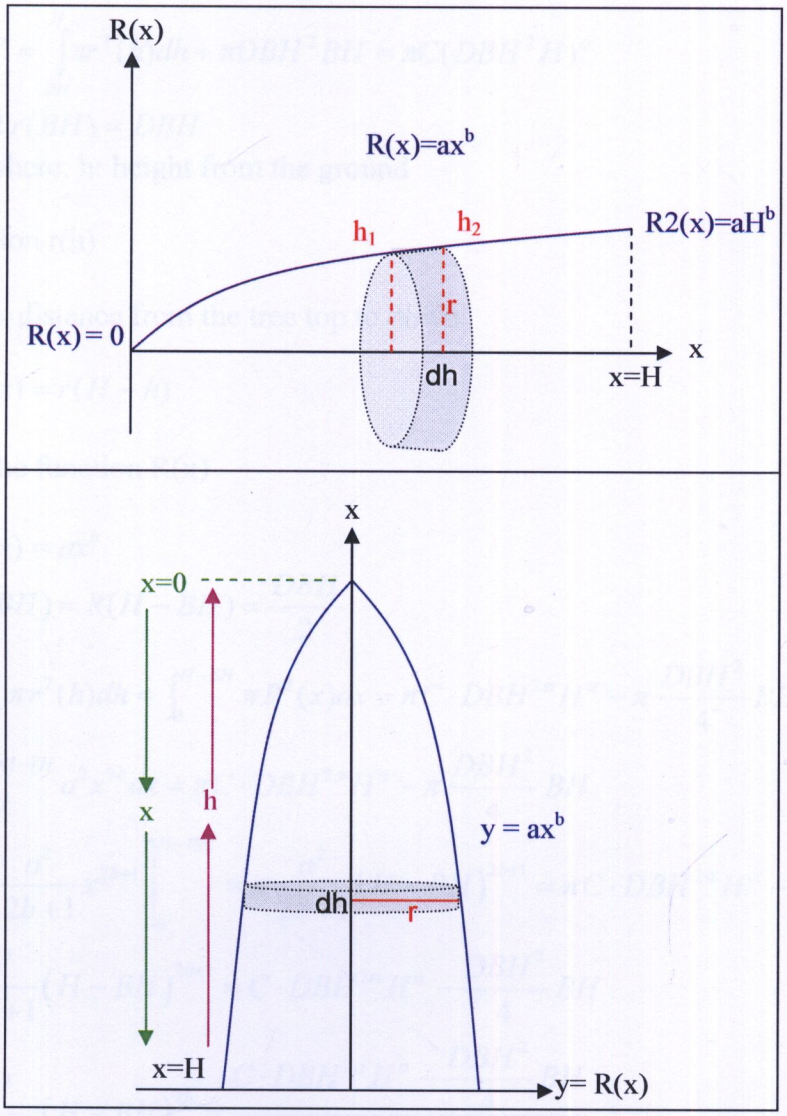

Figure 3.16 The assumptions of function R(x)

How to derive trunk diameter function r(h) or R(x) based on Vs equation was discussed below. Variable x is the distance from the tree top.

Trunk volume of a mangrove tree

$$Vs = 0.0687 \times 10^{0.724} \times (DBH^2 \times H)^{0.931} \quad \text{---------- [3]}$$

where: DBH(m): Diameter at breast height
H(m): Tree height
Vs(m^3): Trunk volume
BH: Breast height (1.3m)

$Vs = \pi C(DBH^2 \times H)^{\alpha}$

$\alpha = 0.931$

$C = 0.115826215$

Tree trunk shape radius r(h) can be obtained from [4].

$$V = \int_{BH}^{H} \pi r^2(h)dh + \pi DBH^2 BH = \pi C(DBH^2 H)^{\alpha}$$

$$2.r(BH) = DBH$$

where: h: height from the ground

Obtain the function r(h)

x = distance from the tree top to down

$$R(x) = r(H - h)$$

Assumption of the function R(x)

$$R(x) = ax^b$$

$$r(BH) = R(H - BH) = \frac{DBH}{2}$$

$$\int_{BH}^{H} \pi r^2(h)dh = \int_0^{H-BH} \pi R^2(x)dx = \pi C \cdot DBH^{2\alpha} H^{\alpha} - \pi \frac{DBH^2}{4} BH$$

$$\pi \int_0^{H-VH} a^2 x^{2b} dx = \pi C \cdot DBH^{2\alpha} H^{\alpha} - \pi \frac{DBH^2}{4} BH$$

$$\pi \left[\frac{a^2}{2b+1} x^{2b+1} \right]_0^{H-BH} = \pi \frac{a^2}{2b+1} (H - BH)^{2b+1} = \pi C \cdot DBH^{2\alpha} H^{\alpha} - \pi \frac{DBH^2}{4} BH$$

$$\frac{a^2}{2b+1} (H - BH)^{2b+1} = C \cdot DBH^{2\alpha} H^{\alpha} - \frac{DBH^2}{4} BH$$

$$\frac{a^2}{2b+1} (H - BH)^{2b} = \frac{C \cdot DBH^{2\alpha} H^{\alpha} - \frac{DBH^2}{4} BH}{H - BH}$$

$$\begin{cases} \frac{a^2}{2b+1} (H - BH)^{2b} = \frac{C \cdot DBH^{2\alpha} H^{\alpha} - \frac{DBH^2}{4} BH}{H - BH} \\ a(H - BH)^b = \frac{DBH}{2} \end{cases}$$

Variable 'a' is one of the constant values of the trunk diameter function R(x). 'a' can be calculated by:

$$a = \frac{DBH}{2} (H - BH)^{-b} \qquad \text{---------- [4]}$$

How to derive constants 'b' of the trunk diameter function R(x) was discussed below.

$$a = \frac{DBH}{2}(H - BH)^{-b}$$

$$\frac{\frac{DBH^2}{4}(H-BH)^{-2b}}{2b+1}(H-BH)^{2b} = \frac{C \cdot DBH^{2\alpha} H^{\alpha} - \frac{DBH^2}{4} BH}{H - BH}$$

$$\frac{\frac{DBH^2}{4}}{2b+1} = \frac{C \cdot DBH^{2\alpha} H^{\alpha} - \frac{DBH^2}{4} BH}{H - BH}$$

$$2b+1 = \frac{H - BH}{C \cdot DBH^{2\alpha} H^{\alpha} - \frac{DBH^2}{4} BH} \frac{DBH^2}{4}$$

$$b = \frac{1}{2}\left(\frac{(H - BH) DBH^2}{4C \cdot DBH^{2\alpha} H^{\alpha} - DBH^2 BH} - 1 \right)$$

$$b = \frac{1}{2}\left(\frac{H - BH}{4C \cdot DBH^{2(\alpha-1)} H^{\alpha} - BH} - 1 \right) \quad \text{---------- [5]}$$

Variable 'b' is another one of the constant values of the trunk diameter function R(x). From rewritten equation, 'b' is calculated by equation [5]. For the assumption of the function $R(x) = ax^b$, 'a' and 'b' is the constant value of tree trunk shape used to illustrate how DBH from ground to tree top change. Afterward, they were utilized to calculate tree volume and project area under water. The functions can be classified into two parts. The first part is served for the tree volume calculation at water level less than or equal to BH (1.3m) illustrated in equation [6]. The second part is used for calculating tree volume at water level higher than 1.3m shown in equation [7]. Similar conditions of two parts are also applied for projected area calculation by equation [8] and [9].

Volume of a mangrove under water (depth = d)

Part 1: when water depth (d) $\leq$ 1.3 meter

$$V_{h<d} = \pi \frac{DBH^2}{4} d \quad \text{---------- [6]}$$

Part 2: when water depth (d) $\geq$ 1.3 meter

$$V_{h>d} = \pi \frac{DBH^2}{4} 1.3 + \pi \left[\frac{a^2}{2b+1} x^{2b+1} \right]_{H-d}^{H-1.3}$$

$$V_{h>d} = \pi \frac{DBH^2}{4} 1.3 + \pi \frac{a^2}{2b+1} ((H-1.3)^{2b-1} - (H-d)^{2b+1}) \quad \text{---------- [7]}$$

Projected area of a mangrove under water (depth = d)

Part 1: when water depth (d) $\leq$ 1.3 meter

$$A_{h<d} = DBH \cdot d \quad \text{---------- [8]}$$

Part 2: when water depth (d) ≥1.3 meter

$$A_{h>d} = DBH \cdot d + \int_{.3}^{d} 2r(h)dh$$

$$= DBH \cdot d + \int_{H-d}^{H-1.3} 2R(x)dx = DBH \cdot d + \int_{H-d}^{H-1.3} 2ax^b dx$$

$$= DBH \cdot d + \left[\frac{2a}{b+1}x^{b+1}\right]_{H-d}^{H-1.3}$$

$$A_{h>d} = DBH \cdot d + \frac{2a}{b+1}((H-1.3)^{b+1} - (H-d)^{b+1}) \quad \text{---------- [9]}$$

The reason why the equation of volume and projected area under water were allocate into 2 parts (water depth (d) ≤ 1.3 m and d > 1.3 meter) are composed of two reasons. First, usually, from the bottom to BH, the diameter is not changing drastically. If use $R(x) = ax^b$ for describe the attribute of trunk diameter like a case1 (see in appendix C), when b is far more than 1, diameter change a lot. For eliminate this limitation, constant diameter from the ground to breast height (BH) was assumed, and construct $R(x) = ax^b$ on d> 1.3 m. Moreover, actually at BH, derivative of the trunk line should be 0 (smoothly connected to the cylinder), but it is not, especially if b is bigger number. That are 2 reasons why equation of volume and projected area under water were allocate into 2 parts.

In additional, a mangroveShape program is developed to solve the equation to obtain parameter a and b by input H and DBH. When obtain a and b, program will compares volume from Komiyama model and integration, as well as DBH given and DBH from function R(x), radius = ax^b (see in source code in appendix G). The mangroveShape provide calculation become easier. The out put look like below.

```
C:\Documents\Dev\mangroveShape\Debug>mangroveShape 6. 0.4
komiyamaShapeAxbCylinder: Volume by Komiyama 0.350309
                          Volume by integration 0.350309
   komiyamaShapeAxbCylinder: DBH given 0.400000   DBH by R(H-h) 0.400000
   komiyamaShapeAxbCylinder: H: 6.00     DBH:0.40 a:0.037618     b:1.079651
          tree id:   1 H:6.00   DBH:0.40      Volume:0.350 axbValid:1
                              a:0.0376183    b:1.07965
```

CHAPTER IV

RESULTS AND DISCUSSION

4.1 Simulation of Canopy Height Model

At first, canopy height model was interpolated from LiDAR by linear equation. The result was illustrated in figure 5.1. By the subtraction of DEM and DSM, Canopy Height Model (CHM) was extracted. The results showed that three-dimensional surface of canopy can be simulated with the pixel size of 50cm. By visualization, each of tree canopies can be readily to see. The surface height was ranging from -0.06 to 10.27m with 1.26m and 2.32m of mean and standard deviation respectively.

Figure 4.1 Canopy height model derived from LiDAR

4.2 Tree parameters estimation from LiDAR

To derive the essential forest parameters (tree position, tree height and crown width), TreeVaW parameter configuration was determined obtaining from the field data observation including: minimum tree height (4.23m), minimum - maximum crown diameter (4.31 and 15.53m). The latter is subsequently used to determine the range of circular window size (19 - 51 pixels) corresponding to the pixel size (50cm).

In addition, the calculation of an appropriate window size to search for tree top is rely on the relationship between tree height and crown width data from the total of 31 trees, field inventory. Using linear regression, crown width equation was constructed to estimate an individual window size when tree height is the independent variable. This equation can determine the appropriate circular filtering window size based on tree height with an R^2 of 0.791. This equation was showed in equation [1]

$$Cw = 1.4334H - 1.7675 \quad \text{---------- [1]}$$

Dependent variables = Crown width (Cw)

Independent variables = Tree Height (Ht)

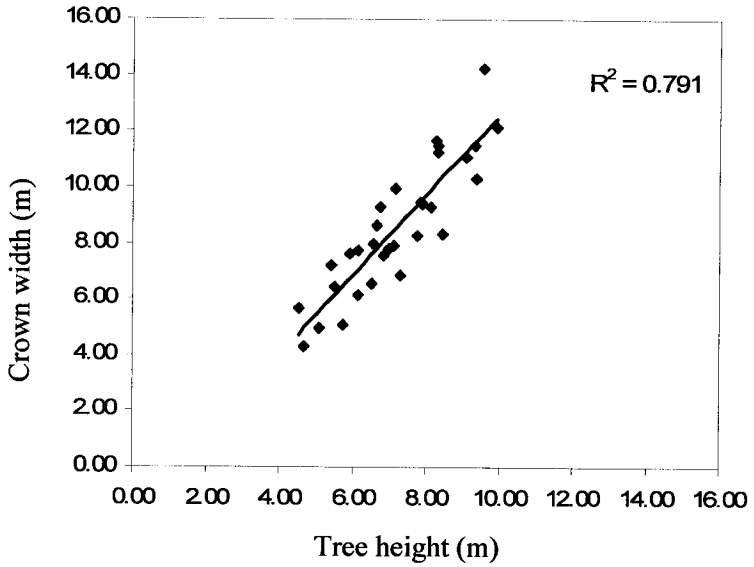

Figure 4.2 The relationship between inventory-crown width and tree height

Tree height has rather positive correlation with crown diameter estimating by linear regression with R^2 of 0.791. The Linear regression statistics show in table 4.1

Table 4.1 Regression statistics

Regression Statistics	
Multiple R	0.889
R Square	0.791
Adjusted R Square	0.784
Standard Error	1.099
Observations	31

The results of tree parameter estimation compose of the tree location, tree height (tree top) and crown diameter. In addition, tree density per unit area can be calculated. In the figure 5.2, the red points represent the tree top (the highest value within tree crown). They also were assumed as the tree location including X and Y coordinate.

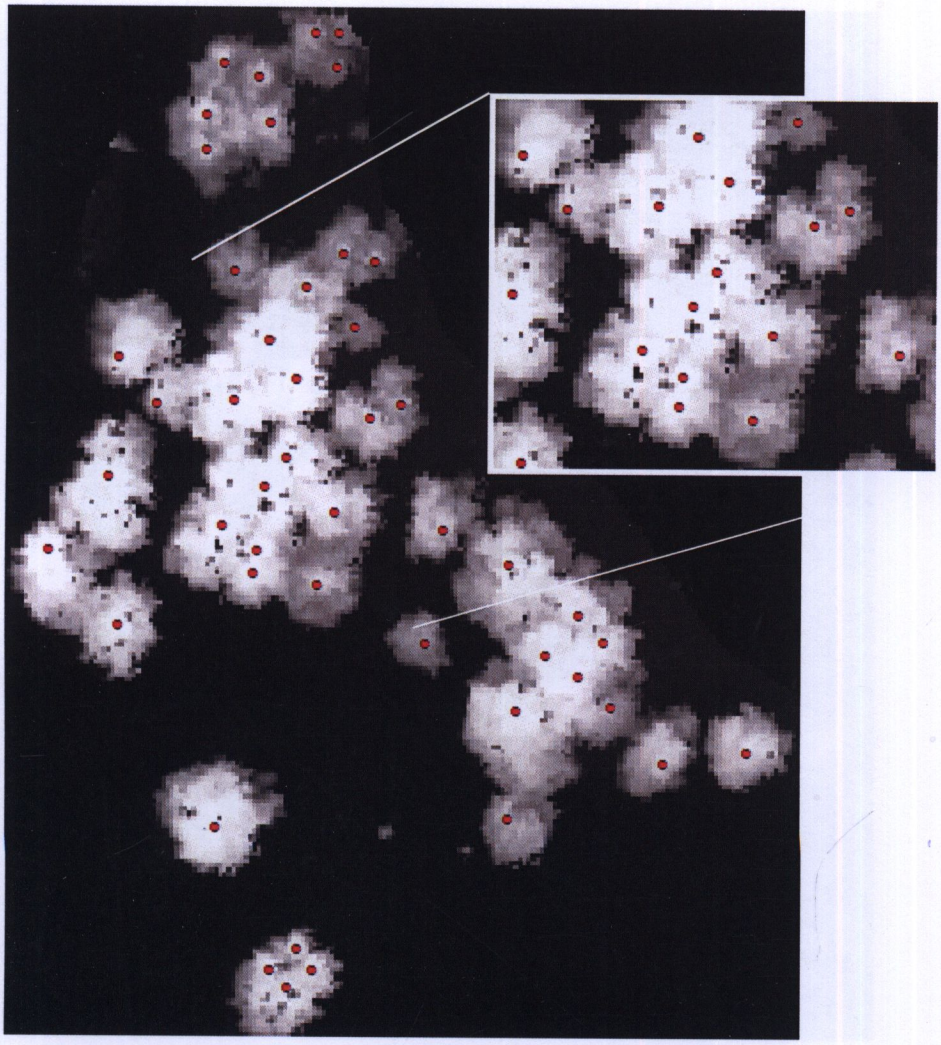

Figure 4.3 The tree position overlay on canopy height model.

Thus, this algorithm for estimating tree height and crown diameter uses a variable window size LM technique that operates under the assumption that there are multiple tree crown shapes and sizes and that the moving LM filter should be adjusted to an appropriate size that corresponds to the spatial structure found on the LiDAR image and on the ground.

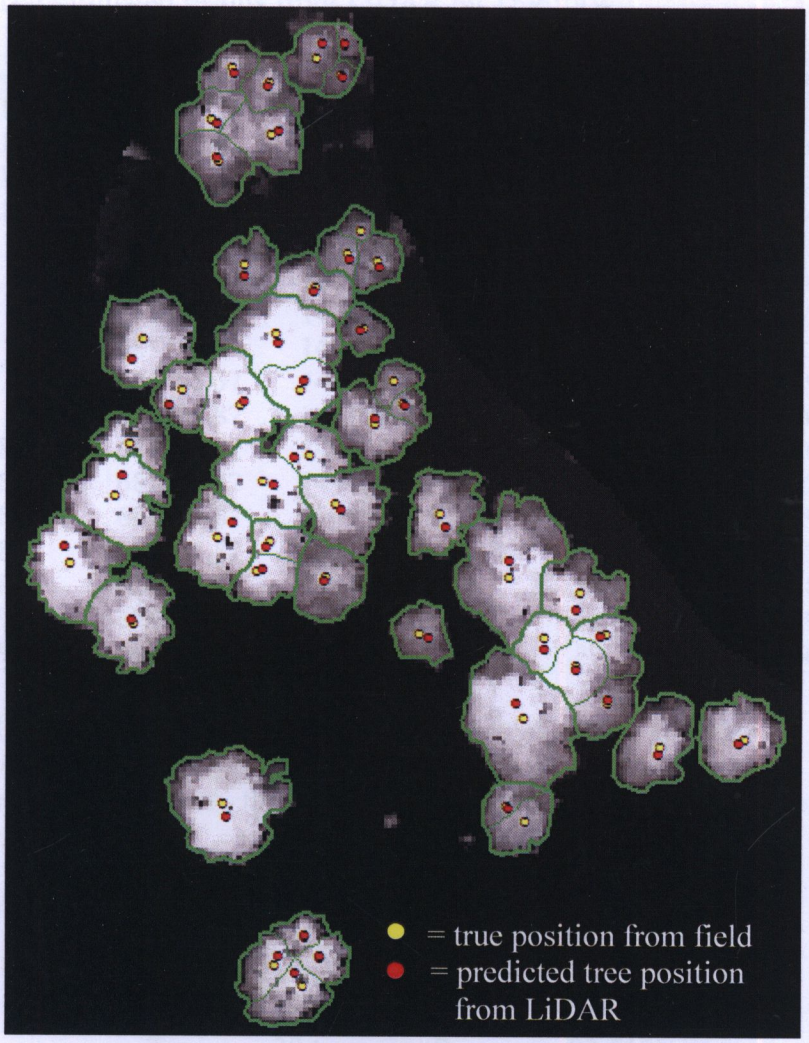

Figure 4.4 The tree position from ground truth and tree position from LiDAR estimation overlay on canopy height model.

As a result of local maximum filtering, tree positions (tree tops) were predicted and illustrated by red circle symbol in figure 4.4. Tree positions (tree tops) measured from the field by GPS were compared with their locations extracted from LiDAR in both directions. The results showed that there are some errors in X and Y distance with an RMSE of 0.155 and 0.290 respectively. However, predicted locations were placed within the crown boundary. The Example of output from tree parameter estimation by TreeVaW

Table 4.2 The estimated results from LiDAR by TreeVaW

Tree ID	X	Y	Crown radius	Height
1/1	681767.58	1493966.31	3.60	8.01
1/2	681769.45	1493964.20	4.63	8.16
1/3	681772.37	1493966.25	6.53	8.25
1/4	681770.60	1493968.78	3.19	7.44
2	681761.37	1493982.75	5.50	9.23
3	681822.37	1493991.75	3.75	7.16
4	681812.87	1493990.25	3.88	6.79
5	681763.37	1494047.25	2.88	5.43
6	681785.37	1494004.25	3.38	5.39
7	681795.87	1493996.25	4.50	8.50
8/1	681759.87	1494061.25	3.63	6.86
8/2	681767.37	1494064.25	3.50	6.82
8/3	681759.87	1494065.25	3.25	7.29
8/4	681761.87	1494071.25	3.13	6.53
8/5	681765.87	1494069.75	2.38	6.18
9/1	681778.87	1494030.25	3.50	6.79
9/2	681782.37	1494031.75	3.00	5.76

To evaluate the effectiveness of estimated tree by LiDAR and ground survey, estimated tree parameters have to be compared with ground-derived tree location, height and crown width number of tree. Then, the correlation coefficient and the RMSE error equation [10] were analyzed.

Table 4.3 Accuracy of tree detection by LiDAR.

Type	Detected	Missing	Accuracy
Tree	30 tree	2	93.55%
Branch	51 branch	4	92.15%

The error is estimated by comparing between tree location, tree height and crown width from ground truth and output from LiDAR.

$$RMSE = \sqrt{\frac{\sum_{i=1}^{n}(X_{esti} - X_{ref})^2}{N}} \qquad \text{---------- [10]}$$

Table4.4 Error estimation of tree's physical parameters by LiDAR

Parameters	RMS Error (m)
X	0.155
Y	0.290
H	0.599
CD	0.781

4.3 DBH Model

As a results of LiDAR extraction from canopy height model, tree height and crown width at individual scale were obtained. To be used in Tsunami run-up model for calculation of the resistance force, effective stem volume and basal area under water level are the critical parameters. For the first one, common allometric model of Komiyama (A. Komiyama et al., 2005) must be discussed. In this model, DBH is considered as an independent factor which is not directly extracted from LiDAR or Canopy Height Model. To derive DBH model, the relationship of crown width, tree height and DBH from field inventory (30 samples) have to be investigated. Afterward, linear regression equation with R^2 (0.91), Standard Error (2.0) was constructed depicted in equation [11]. TH

$$DBH=1.801Cw+1.677H-4.583 \text{ ---------- } [11]$$

where: Cw = crown width (m)
H = Tree Height (m)

DBH from observe and predicted by LiDAR show in Appendix 2. The LiDAR predicted DBH and field- measured DBH from correlate well with an R^2 value of 0.819 (Figure 4.5)

Table 4.5 Linear regression statistics of DBH Model

Regression Statistics	
Multiple R	0.95
R Square	0.91
Adjusted R Square	0.90
Standard Error	2.00

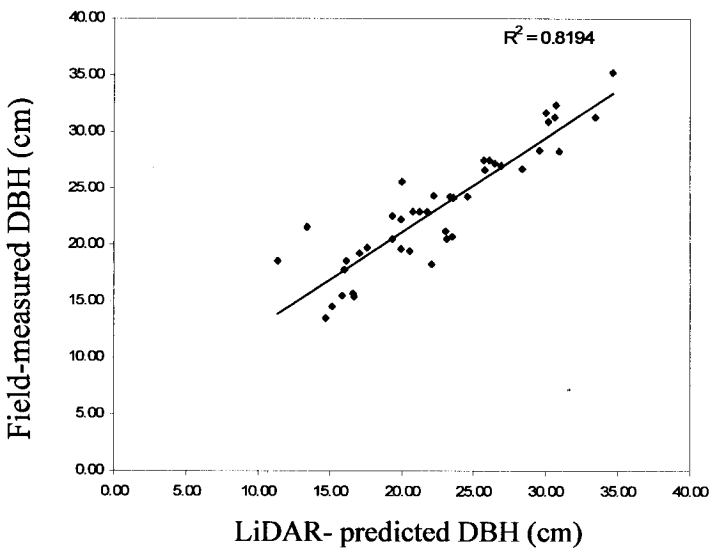

Figure 4.5 Predicted vs. field- measured DBH

4.4 Trunk diameter function

Constant value of a and b were derived from function of $R(x) = ax^b$ after solving trunk diameter function. Couple derived values, a and b acquired from equation [4], [5]

respectively were capable to explain shape, size of tree trunk attributes corresponding to tree height (x). Practically, trunk diameter function were applied to 52 trees in the study plot to calculate a and b. The results were summarized in appendix D. Table 4.6 provides the examples of tree trunk attributes and trunk shape graph shown in figure 4.6 .

Table 4.6 The information and a, b value of mangrove tree

TREE ID	H	DBH	a	b
3	8.25	0.33	0.03090	0.86046

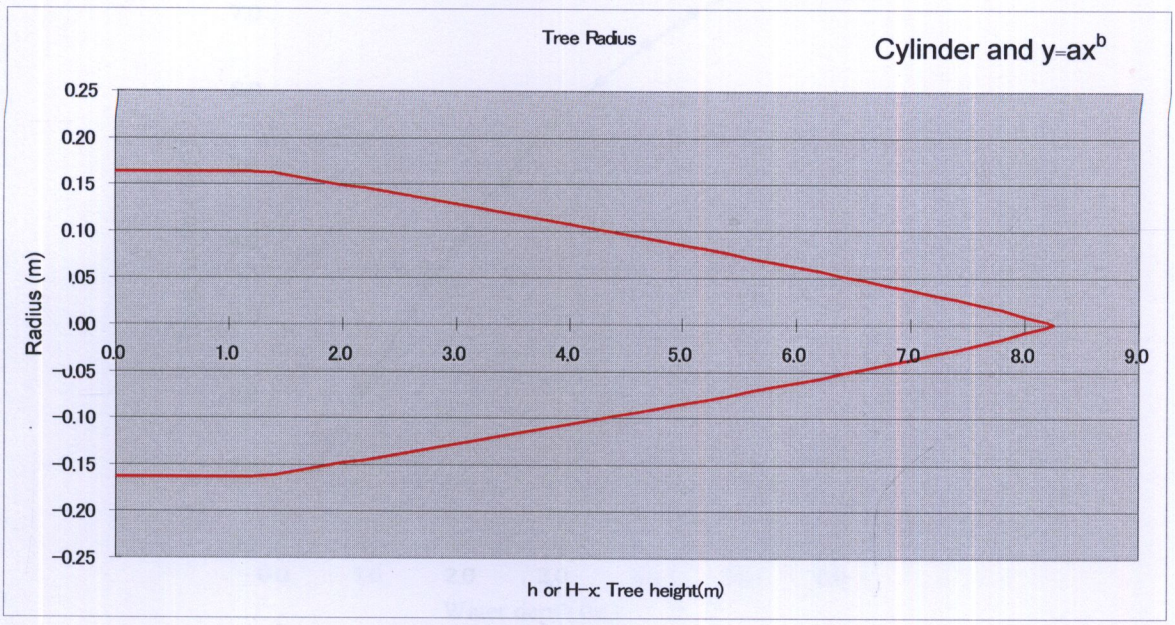

Figure 4.6 Trunk shape line graph of mangrove tree by function of Cylinder and $R(x) = ax^b$

4.5 Trunk volume

There are two cases for calculation of trunk volume regarding the equation [6] and [7]. The first case is served for the height lower than the DBH measurement (1.3m) which the trunk shape was assumed as cylinder. Another case is devoted for the height higher than the DBH measurement (1.3m) with the assumption of $y= ax^b$ (x-H-h). Table 4.7 summarizes the outputs trunk volume along the water depth with interval 0.5m ranging from 0-5m. The integration trunk volume deriving from established function is similar to the volume calculated by Komiyama volume model.

Table 4.7 Trunk volume (m^3) the water level with interval 0.5m

T_ID	H	DBH	a	B	V(0.5)	V(1.0)	V(1.5)	V(2.0)	V(2.5)	V(3.0)	V(3.5)	V(4.0)	V(4.5)	V(5.0)
1.1	8.01	0.22	0.02576	0.75826	0.0187	0.0374	0.0559	0.0727	0.0876	0.1005	0.1116	0.1210	0.1288	0.1350
1.2	8.16	0.26	0.02775	0.79746	0.0261	0.0522	0.0780	0.1015	0.1221	0.1399	0.1552	0.1681	0.1788	0.1874
1.3	8.25	0.33	0.03090	0.86046	0.0422	0.0844	0.1261	0.1637	0.1965	0.2247	0.2486	0.2686	0.2849	0.2979
1.4	7.44	0.19	0.02503	0.74601	0.0148	0.0295	0.0441	0.0573	0.0688	0.0787	0.0870	0.0939	0.0995	0.1038
2	9.23	0.31	0.02846	0.81401	0.0370	0.0741	0.1108	0.1445	0.1745	0.2012	0.2246	0.2449	0.2623	0.2769
3	7.16	0.21	0.02647	0.77751	0.0172	0.0344	0.0514	0.0666	0.0797	0.0908	0.0999	0.1074	0.1132	0.1175

4	6.79	0.21	0.02695	0.79252	0.0170	0.0339	0.0507	0.0655	0.0780	0.0885	0.0969	0.1036	0.1086	0.1121
6	5.39	0.17	0.02615	0.82134	0.0109	0.0217	0.0324	0.0414	0.0484	0.0537	0.0575	0.0599	0.0613	0.0618
7	8.50	0.28	0.02819	0.80608	0.0301	0.0602	0.0900	0.1171	0.1411	0.1620	0.1801	0.1955	0.2084	0.2189

Trend line in figure 4.7 illustrates the relationship of water depth and total trunk volume for separated interval (0.5m). The rate of change of trunk volume rapidly increase and gradually decease when the water depth increase (inversely increase of tree height).

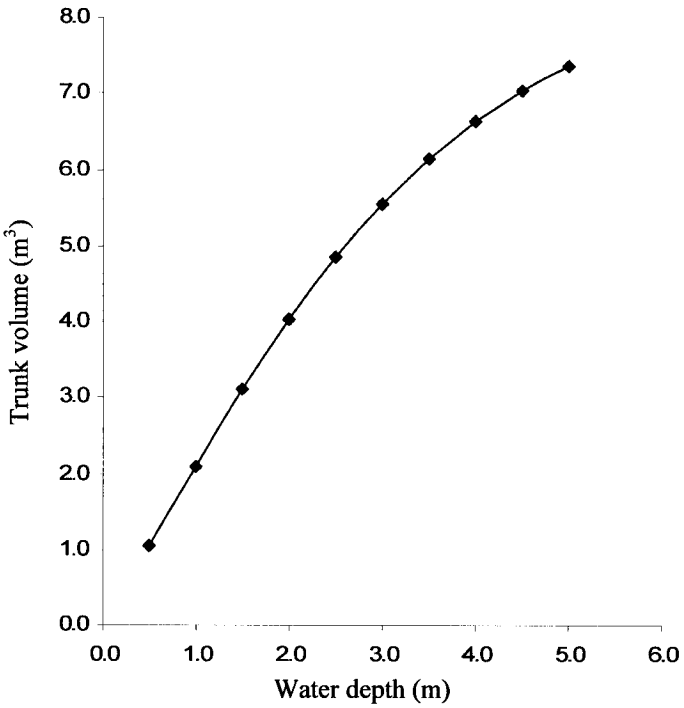

Figure 4.7 Relationship between total trunk volume and water depth

4.6 Projected area

The projected areas along the along the water depth were calculated by equation [8] and [9] belonging the two different cases similar in the trunk volume. Table 4.8 shows some example outputs of projected area at each interval. Figure 4.8 illustrates the relationship of water depth with interval 0.5m and total projected area. The rate of change of projected area correlating with the change of water depth is similar in the case of trunk volume.

Table4.8 Table projected area under the water level with interval 0.5m

TreeID	A(0.5)	A(1.0)	A(1.5)	A(2.0)	A(2.5)	A(3.0)	A(3,5)	A(4.0)	A(4.5)	A(5.0)	A(H)
1.1	0.109	0.218	0.314	0.386	0.454	0.517	0.576	0.630	0.679	0.723	0.865
1.2	0.129	0.258	0.370	0.455	0.534	0.608	0.677	0.739	0.796	0.847	1.017
1.3	0.164	0.328	0.470	0.576	0.675	0.766	0.851	0.928	0.998	1.060	1.263
1.4	0.097	0.194	0.279	0.343	0.403	0.458	0.509	0.556	0.598	0.634	0.730
2	0.154	0.307	0.441	0.542	0.638	0.728	0.812	0.890	0.963	1.029	1.326
3	0.105	0.209	0.301	0.369	0.433	0.491	0.544	0.592	0.634	0.671	0.752
4	0.104	0.208	0.299	0.366	0.428	0.484	0.535	0.580	0.619	0.652	0.711
6	0.083	0.166	0.239	0.291	0.337	0.377	0.410	0.438	0.458	0.470	0.474
7	0.138	0.277	0.398	0.489	0.574	0.654	0.728	0.796	0.859	0.915	1.123

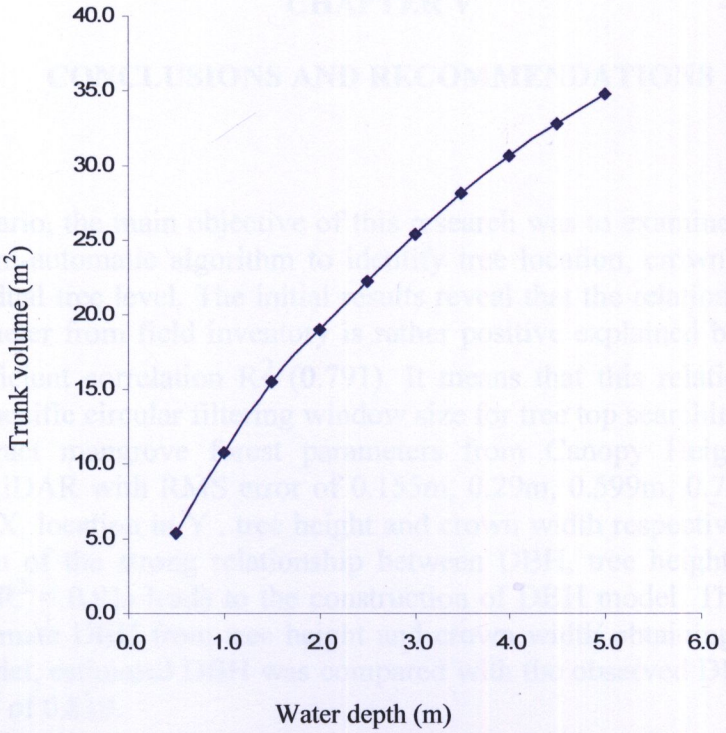

Figure 4.8 Relationship between total projected area and water depth

Table 4.9 Mangrove forest plot volume and projected area

Height level (m)	Volume(m^3)	Projected Area (m^2)
0.5	1.0386	5.3976
1.0	2.0772	10.7951
1.5	3.1057	15.5100
2.0	4.0327	19.0300
2.5	4.8416	22.3021
3.0	5.5392	25.3212
3.5	6.1326	28.0809
4.0	6.6292	30.5740
4.5	7.0370	32.7908
5.0	7.3645	34.7292
Total	8.1878	41.3487

The conclusion of trunk volume and projected area at plot scale is provided in table 4.9. It reveals that separated trunk volume starts from 1 m^3 at 0.5m water depth to 7.36 m^3 at 5m. The total plot trunk volume is approximately 8.187 m^3. In similar, separated projected area is ranging from 5.39 m^2 to 34.72 m^2 along the ground to 5m with the total plot projected area about 41.348 m^2. In case of estimated DBH, the total plot and mean plot equal to 10.80m and 22.97cm respectively.

CHAPTER V

CONCLUSIONS AND RECOMMENDATIONS

5.1 Conclusion

In the first scenario, the main objective of this research was to examine the application of LiDAR and semi-automatic algorithm to identify tree location, crown diameter and tree height at individual tree level. The initial results reveal that the relationship of tree height and crown diameter from field inventory is rather positive explained by linear regression with high coefficient correlation R^2 (0.791). It means that this relation can be used to determine the specific circular filtering window size for tree top searching. In addition, it is capable to extract mangrove forest parameters from Canopy Height Model (CHM) deriving from LiDAR with RMS error of 0.155m, 0.29m, 0.599m, 0.781cm according to tree location in X, location in Y , tree height and crown width respectively. Consequently, the investigation of the strong relationship between DBH, tree height and crown width from the field (R^2 = 0.91) leads to the construction of DBH model. The objective of this model is to estimate DBH from tree height and crown width obtaining from LiDAR. To validate the model, estimated DBH was compared with the observed DBH resulting in the positive with R^2 of 0.819.

In the second scenario, trunk diameter function for simulating the tree trunk shape and calculating the attributes of mangrove tree was developed and investigated based on the assumption of cylinder model and $R(x) = ax^b$ model. The examination of results express that trunk diameter function has a potential to calculate trunk volume and projected are under water level. Following outcomes will be further used to calculate the resistant force against Tsunami wave in the Tsunami run-up model. Finally, MangroveShape program developed in this research makes the users to calculate the significant parameters easily.

5.2 Recommendation for the future works

The proposed methodology to achieve the targets is quite well. However, there are some critical issues that are possible to improve the accuracy and reliability of the results.

1. The algorithm for tree parameter exaction (TreeVaW) is developed only for plantation pine tree. So there are some effects when applying to mangrove tree. The new algorithms based directly on the mangrove tree are needed.
2. In the nature, tree height can not estimate crown diameter with the high accuracy in various environments. To avoid the error, the algorithm for direct crown diameter measurement on the image is requested.
3. The common LiDAR usually is capable to measure only the object height on the land surface. It cannot penetrate the water through the seabed. So, the height of tree part that has been submerged cannot be measured. The new technology of LiDAR accompanying with multiple return both from the ground and seabed is preferable to achieve the exact tree height.
4. The characteristics of mangrove tree vary in the variety of environments. The outcomes of this research will be used to calculate the resistant force by Tsunami run-up model. So, the study site should be some areas that are susceptible to Tsunami.
5. If there is a function of a total volume (VS-+VB+VL) of using DBH and H, then same equation can be applied

Reference

Blair JB, Hofton MA.1999.Modeling laser altimeter return waveforms over complex vegetation using high-resolution elevation data.Geophysical Research Letters 26:2509–2512.

Brandtberg T, Warner TA, Landenberger RE, McGraw JB. 2003. Detection and analysis of individual leaf-off tree crowns in small footprint, high sampling density LiDAR data from the eastern deciduous forest in North America. Remote sensing of environment, v85, p290.

Dubayah R, Blair JB, Bufton JL, Clark DB, JaJa J, Knox R, Luthcke SB, Prince S, Weishampel J., (1997) The vegetation canopy LiDAR mission. Pages 100-112 in Proceedings of Land Satellite Information in the Next Decade, II: Sources and Applications. Bethesda (MD): American Society of Photogrammetry and Remote Sensing.

Dubayah, Ralph O. Drake, Jason B., (2000), LiDAR Remote Sensing for Forestry, Journal of Forestry, Volume 98, Number 6, 1 June 2000, pp. 44-46(3)

Friedlaender, H. and Koch, B., 2000. First experience in the application of laser scanner data for the assessment of vertical and horizontal forest structures. *International Archives of Photogrammetry and Remote Sensing*, 33(B7).

H. Balzter, C.S. Rowland and P. Saich (2007) Forest canopy height and carbon estimation at Monks Wood National Nature Reserve, UK, using dual-wavelength SAR interferometry, Remote Sensing of Environment, In Press, Corrected Proof, Available online 26 December 2006.

H. J. Zwally, B. Schutz, W. Abdalati, J. Abshire, C. Bentley, A. Brenner, J. Bufton, J. Dezio, D. Hancock, D. Harding, et al., (2002) ICESat's laser measurements of polar ice, atmosphere, ocean, and land, Journal of Geodynamics, Volume 34, Issues 3-4, October-November 2002, Pages 405-445

HONDA Kiyoshi. Forest for Tsunami Disaster Mitigation. PowerPoint presentation, Asian Institute of Technology, 2008

J. Bryan Blair, David L. Rabine and Michelle A. Hofton (1999) The Laser Vegetation Imaging Sensor: a medium-altitude, digitisation-only, airborne laser altimeter for mapping vegetation and topography, ISPRS Journal of Photogrammetry and Remote Sensing, Volume 54, Issues 2-3, July 1999, Pages 115-122

Japan wildlife research center. Development of Tsunami energy mitigation efficiency calculation program. Tsunami manual, 2007;25(1)1-25

Jason B. Drake, Ralph O. Dubayah, David B. Clark, Robert G. Knox, J. Bryan Blair, Michelle A. Hofton, Robin L. Chazdon, John F. Weishampel and Steve Prince, (2002), Estimation of tropical forest structural characteristics using large-footprint LiDAR, Remote Sensing of Environment, Volume 79, Issues 2-3, February 2002, Pages 305-319

Kalogirou, V. (2006) Simulation of Discrete-return LiDAR signal from conifer stands for forestry applications, MSc Thesis (University of London MSc in Remote Sensing), University College London, September 2006.

KENJI HARADA, FUMIHIKO IMAMURA: Effects on Coastal Forest on Tsunami Hazard Mitigation – A Preliminary Investigation

Kenji HARADA, Latief Hamzah, Fumihiko Imamura: Study on the Mangrove Control Forest to Reduce Tsunami Impact

Kenji HARADA, Yoshiaki KAWATA. Study on Tsunami Reduction Effect of Coastal Forest due to Forest Growth, Annuals of Disaster Prevention Research Institute, Kyoto University, NO. 48C, 2005

Koetz, B.; Morsdorf, F.; Sun, G.; Ranson, K.J.; Itten, K.; Allgower, B., "Inversion of a LiDAR waveform model for forest biophysical parameter estimation," Geoscience and Remote Sensing Letters, IEEE , vol.3, no.1pp. 49- 53, Jan. 2006

Lefsky MA, Cohen WB, Acker SA, Parker GC, Spies TA, Harding D. 1999. LiDAR remote sensing of the canopy structure and biophysical properties of Douglas-fir western hemlock forests. Remote Sensing of Environment, vol 70, p 338-361.

Lewis , P. (1999) The Botanical Plant Modelling System. Agronomie: Agriculture and Environment Vol.19, No.3-4, pp.185-210

Lim, K, Treitz, P., Wulder, M., St-Onge, B., and Flood, M., (2003) LiDAR remote sensing of forest structure, *Progress in Physical Geography*, **27**, 1, pp. 88-106.

Lovell JL, Jupp DLB, Calvenor DS, Coops NC. 2003. Using airborne and ground-based ranging LiDAR to measure canopy structure in Australian forests. Canadian journal of remote sensing, v29, p607.

M. A. Hofton, L. E. Rocchio, J. B. Blair and R. Dubayah (2002) Validation of Vegetation Canopy LiDAR sub-canopy topography measurements for a dense tropical forest, Journal of Geodynamics, Volume 34, Issues 3-4, October-November 2002, Pages 491-502

Ni-Meister, W.; Jupp, D.L.B.; Dubayah, R., "Modeling LiDAR waveforms in heterogeneous and discrete canopies," Geoscience and Remote Sensing, IEEE Transactions on , vol.39, no.9pp.1943-1958, Sep 2001

Peter Hyde, Ross Nelson, Dan Kimes and Elissa Levine (2007) Exploring LiDAR–RaDAR synergy—predicting aboveground biomass in a southwestern ponderosa pine forest using LiDAR, SAR and InSAR Remote Sensing of Environment, Volume 106, Issue 1, 15 January 2007, Pages 28-38

Peter Hyde, Ralph Dubayah, Wayne Walker, J. Bryan Blair, Michelle Hofton and Carolyn Hunsaker (2006) Mapping forest structure for wildlife habitat analysis using multi-sensor (LiDAR, SAR/InSAR, ETM+, Quickbird) synergy, Remote Sensing of Environment, Volume 102, Issues 1-2, 30 May 2006, Pages 63-73

P. Lewis and M. Disney (Nov 2006 Submitted; Jan 2007 Accepted) Spectral invariants and scattering across multiple scales from within-leaf to canopy, Remote Sensing of Environment.

Popescu SC, Ananth U. Kini.TREEVAW: a versatile tool for analyzing forest canopy LiDAR data – A preview with an eye towards future. Department of Computer Science Texas A & M University

Popescu SC, Wynne RH, Nelson RH. Estimating plot-level tree heights with LIDAR: local filtering with a canopy-height based variable window size. Computers and Electronics in Agriculture, 2002; 37(1-3): 71-95

Popescu SC, Wynne RH, Nelson RH. Measuring individual tree crown diameter with LIDAR and assessing its influence on estimating forest volume and biomass. Canadian Journal of Remote Sensing, 2003; 29(5):564-77.

Popescu SC, Wynne RH. Seeing the trees in the forest: using LIDAR and multispectral data fusion with local filtering and variable window size for estimating tree height. Photogrammetric Engineering & Remote Sensing 2004; 70(5):589-604.

Q. Sun and K. J. Ranson, "Modeling LiDAR returns from forest canopies," IEEE Trans. Geosci. Remote Sens., vol. 38, no. 6, pp. 2617–2626, Jun. 2000.

Ralph Dubayah, Bryan Blair, Jack Bufton et al. The vegetation canopy LiDAR mission. http://www.geog.umd.edu/vcl/vcltext.html#rationale.

S. Y. Kotchenova, N. V. Shabanov, Y. Knyazikhin, A. B. Davis, R. Dubayah, and R. B. Myneni, Modeling LiDAR waveforms with time-dependent stochastic radiative transfer theory for remote estimations of forests structure. *Journal of Geophysical Research*, 108 (D15), 2003.

Tetsya Hiraishi, Kenji HARADA(2003): Greenbelt Tsunami Prevention in South-Pacific Region, Report of the Port and Airport Research Institute Vol. 42, No.2 (June 2003), pp.1-23

Todd KW, Csillag F, Atkinson PM. 2003. Three dimensional mapping of light transmittance and foliage distribution using LiDAR. Canadian journal of remote sensing, v29, p544

Y. Govaerts, (1996) A Model of Light Scattering in Three-Dimensional Plant Canopies: A Monte Carlo Ray Tracing Approach. *PhD thesis*, Ispra, Italy: Space Applicat. Inst. JRC, 1996.

Y. Imai, M. Setojima,Y. Yamagishi,N. Fujiwara. Tree height measuring characteristics of forest by LiDAR data difference in resolution. National Institute for Land and Infrastructure Management

Appendices A

GPS points and tree parameters from field inventory

Point type		UTM coordinates, zone 47, WGS84						
No.	Tree ID*	X	Y	Cw1 (m)	Cw2 (m)	Cw avg (m)	H (m)	DBH (cm)
1	1.1	681766.98	1493965.11	9.08	5.30	7.19	8.01	26.85
2	1.2	681770.41	1493962.60	11.00	7.51	9.25	8.16	26.67
3	1.3	681772.38	1493966.06	6.35	6.70	6.53	8.25	24.31
4	1.4	681770.68	1493968.48	7.43	5.30	6.37	7.44	25.54
5	2	681760.88	1493984.27	11.03	12.23	11.63	8.28	32.31
6	3	681823.15	1493992.14	10.00	9.84	9.92	7.15	27.03
7	4	681812.92	1493991.16	9.56	9.00	9.28	6.78	29.56
8	6	681784.19	1494004.51	6.67	11.58	9.13	5.42	15.67
9	7	681796.83	1493994.54	14.62	13.06	13.84	8.50	35.22
10	8.1	681760.06	1494060.69	9.65	5.50	7.58	6.86	22.20
11	8.2	681766.42	1494063.96	9.82	8.82	9.32	6.82	25.89
12	8.3	681759.20	1494065.75	5.55	8.11	6.83	7.29	24.45
13	8.4	681761.62	1494072.02	5.98	7.11	6.54	6.53	19.75
14	8.5	681766.15	1494070.10	7.82	7.68	7.75	6.18	18.53
15	9.1	681778.85	1494029.48	9.52	10.48	10.00	6.79	25.60
16	9.2	681782.35	1494031.91	5.13	4.95	5.04	5.75	15.45
17	9.3	681781.21	1494034.71	6.37	6.49	6.43	5.54	15.40
18	10	681763.31	1494048.57	7.83	7.62	7.72	5.24	15.34
19	11.1	681775.58	1494049.79	9.07	9.67	9.37	5.70	16.57
20	11.2	681777.16	1494052.51	5.01	4.81	4.91	5.10	15.67
21	11.3	681779.21	1494048.85	6.70	5.55	6.13	6.16	13.44
22	12	681777.57	1494040.95	5.36	5.97	5.67	4.53	21.55
23	13	681751.25	1494039.55	11.33	11.63	11.48	8.32	27.28
24	14.1	681762.73	1494031.89	12.56	15.86	14.21	9.58	23.30
25	14.2	681755.93	1494033.66	7.11	8.68	7.89	7.11	18.65
26	15	681750.10	1494005.69	9.88	12.56	11.22	8.34	30.46
27	16	681742.59	1494012.90	12.60	9.52	11.06	9.09	31.27
28	17	681786.72	1494018.79	9.47	8.44	8.96	6.55	32.25
29	18	681747.94	1494020.88	11.00	11.97	11.48	9.35	35.64
30	19	681749.63	1494027.12	5.39	8.53	6.96	7.73	26.68
31	20.1	681769.88	1494033.56	7.83	9.67	8.75	10.02	25.89
32	20.2	681767.16	1494040.27	8.68	15.65	12.16	9.91	28.55
33	21	681771.86	1494045.85	9.21	6.41	7.81	6.99	18.23
34	22.1	681771.81	1494072.95	7.78	6.55	7.17	5.42	19.23
35	22.2	681774.74	1494071.12	4.55	4.08	4.31	4.67	18.57
36	22.3	681775.18	1494074.71	7.21	9.61	8.41	4.23	14.55
37	23	681773.15	1494011.25	9.28	8.03	8.65	6.67	17.45
38	24	681774.27	1494019.92	9.48	9.27	9.38	7.93	30.12

Point type		UTM coordinates, zone 47, WGS84						
No.	Tree ID*	X	Y	Cw1 (m)	Cw2 (m)	Cw avg (m)	H (m)	DBH (cm)
39	25	681760.09	1494015.89	8.85	11.74	10.30	9.36	28.41
40	26.1	681766.40	1494015.63	6.87	7.34	7.11	8.86	21.11
41	26.2	681764.88	1494011.96	9.05	6.20	7.63	8.34	20.50
42	27.1	681765.50	1494022.63	12.78	4.21	8.49	10.21	26.72
43	27.2	681771.02	1494025.71	6.59	8.15	7.37	9.99	27.24
44	28.1	681799.24	1494004.18	7.54	6.62	7.08	8.37	28.32
45	28.2	681802.90	1494000.89	8.44	8.25	8.34	8.44	24.23
46	28.3	681806.45	1494004.53	9.07	7.44	8.26	7.78	27.25
47	28.4	681806.71	1493996.36	6.93	9.07	8.00	6.56	27.87
48	29	681794.89	1494011.34	14.05	17.00	15.53	8.42	38.29
49	30	681803.33	1494009.58	10.09	8.85	9.47	7.86	27.48
50	31.1	681796.85	1493982.25	0.00	0.00	5.00	5.81	14.57
51	31.2	681794.70	1493984.11	5.42	7.69	7.59	6.55	17.77

Tree ID – ID of tree, the number before decimal is ID of trees, the number after decimal is ID of main branch; Cw1 – crown width in north to south direction; Cw2 – crown width in east to west direction; Cw avg – average crown width of measurements Cw1 and Cw2; H – tree height; DBH – diameter of trees trunk (measured at breast height)

AppendixB. Comparing between tree position and parameters from field measurements and predicted from LiDAR.

No.	Tree ID	Tree position from field		Tree position from simulation		Crown diameter		Tree height		DBH	
		X	Y	X	Y	Field	Simulation	Field	Simulation	Field	Simulation
1	1.1	681766.98	1493965.11	681767.58	1493966.31	7.19	7.20	8.21	8.01	26.85	21.81697
2	1.2	681770.41	1493962.60	681769.45	1493964.20	9.25	9.26	8.26	8.16	26.67	25.77858
3	1.3	681772.38	1493966.06	681772.37	1493966.25	6.53	13.06	8.45	8.25	24.31	32.77331
4	1.4	681770.68	1493968.48	681770.60	1493968.78	6.37	6.38	7.64	7.44	25.54	19.38426
5	2	681760.88	1493984.27	681761.37	1493982.75	11.63	11.00	8.28	9.23	32.31	30.70671
6	3	681823.15	1493992.14	681822.37	1493991.75	9.92	7.50	7.55	7.16	27.03	20.93182
7	4	681812.92	1493991.16	681812.87	1493990.25	9.28	7.76	6.88	6.79	29.56	20.77959
8	6	681784.19	1494004.51	681785.37	1494004.25	9.13	6.76	5.42	5.39	15.67	16.63079
9	7	681796.83	1493994.54	681795.87	1493996.25	13.84	10.00	8.80	8.50	35.22	27.6815
10	8.1	681760.06	1494060.69	681759.87	1494061.25	7.58	7.26	6.86	6.86	22.20	19.99648
11	8.2	681766.42	1494063.96	681767.37	1494064.25	9.32	8.00	6.82	6.82	25.89	21.26214
12	8.3	681759.20	1494065.75	681759.87	1494065.25	6.83	6.50	7.45	7.29	24.45	19.34883
13	8.4	681761.62	1494072.02	681761.87	1494071.25	6.54	6.26	6.73	6.53	19.75	17.64207
14	8.5	681766.15	1494070.10	681765.87	1494069.75	7.75	5.76	6.15	6.18	18.53	16.15462
15	9.1	681778.85	1494029.48	681778.87	1494030.25	10.00	7.34	6.89	6.79	25.60	20.02317
16	9.2	681782.35	1494031.91	681782.37	1494031.75	5.04	6.00	5.95	5.76	15.45	15.88252
17	9.3	681781.21	1494034.71	-	-	6.43	-	5.54	-	15.40	
18	10	681763.31	1494048.57	681763.37	1494047.25	7.72	6.76	5.24	5.43	15.34	16.69787
19	11.1	681775.58	1494049.79	681775.87	1494049.25	9.37	7.50	5.70	6.56	16.57	19.92562
20	11.2	681777.16	1494052.51	-	-	4.91		5.10		15.67	
21	11.3	681779.21	1494048.85	681779.37	1494048.25	6.13	5.00	6.26	6.16	13.44	14.75232
22	12	681777.57	1494040.95	681777.13	1494040.66	5.67	5.76	4.53	4.54	21.55	13.40434
23	13	681751.25	1494039.55	681749.87	1494037.25	11.48	12.00	8.52	8.31	27.28	30.96487

No.	Tree ID	Tree position from field		Tree position from simulation		Crown diameter		Tree height		DBH	
		X	Y	X	Y	Field	Simulation	Field	Simulation	Field	Simulation
24	14.1	681762.73	1494031.89	681763.37	1494032.25	14.21	12.20	9.98	9.70	23.30	33.6561
25	14.2	681755.93	1494033.66	681754.37	1494031.75	7.89	9.00	7.41	7.11	18.65	23.54947
26	15	681750.10	1494005.69	681749.87	1494006.25	11.22	9.26	8.34	8.35	30.46	26.09721
27	16	681742.59	1494012.90	681741.87	1494014.75	11.06	12.62	9.09	9.15	31.27	33.49017
28	17	681786.72	1494018.79	681787.37	1494017.25	8.96	7.26	6.75	6.57	32.25	19.51015
29	18	681747.94	1494020.88	681748.87	1494023.25	11.48	10.50	9.40	9.36	35.64	30.02422
30	19	681749.63	1494027.12	-	-	6.96	-	7.73	-	26.68	
31	20.1	681769.88	1494033.56	681770.37	1494034.75	8.75	10.00	10.42	10.02	25.89	30.23054
32	20.2	681767.16	1494040.27	681767.37	1494039.25	12.16	13.50	9.98	9.91	28.55	36.34957
33	21	681771.86	1494045.85	681771.60	1494045.37	7.81	7.80	6.99	7.54	18.23	22.10938
34	22.1	681771.81	1494072.95	681772.37	1494074.75	7.17	7.00	5.50	5.42	19.23	17.11334
35	22.2	681774.74	1494071.12	681774.87	1494070.75	4.31	4.50	4.57	4.67	18.57	11.35309
36	22.3	681775.18	1494074.71	681775.18	1494074.91	8.41	6.92	4.23	4.37	14.55	15.20841
37	23	681773.15	1494011.25	681772.87	1494010.75	8.65	7.76	6.97	6.68	17.45	20.59512
38	24	681774.27	1494019.92	681774.87	1494019.25	9.38	8.26	7.93	7.94	30.12	23.60864
39	25	681760.09	1494015.89	681761.88	1494017.77	10.30	10.30	9.36	9.31	28.41	29.58017
40	26.1	681766.40	1494015.63	681765.93	1494014.94	7.11	7.12	8.99	8.86	21.11	23.09834
41	26.2	681764.88	1494011.96	681765.59	1494012.15	7.63	7.62	8.74	8.34	20.50	23.1268
42	27.1	681765.50	1494022.63	681766.87	1494022.25	8.49	8.76	10.21	10.27	26.72	28.41655
43	27.2	681771.02	1494025.71	681769.29	1494025.63	7.37	7.96	10.11	9.98	27.24	26.48942
44	28.1	681799.24	1494004.18	681799.09	1494002.91	7.08	7.08	8.40	8.37	28.32	22.20457
45	28.2	681802.90	1494000.89	681802.87	1494000.25	8.34	8.34	8.74	8.44	24.23	24.59122
46	28.3	681806.45	1494004.53	681805.86	1494004.35	8.26	8.26	7.82	7.78	27.25	23.34032
47	28.4	681806.71	1493996.36	681806.69	1493996.76	8.00	8.00	6.71	6.56	27.87	20.82612
48	29	681794.89	1494011.34	681794.87	1494013.25	15.53	11.62	8.62	8.53	38.29	30.64943

No.	Tree ID	Tree position from field		Tree position from simulation		Crown diameter		Tree height		DBH	
		X	Y	X	Y	Field	Simulation	Field	Simulation	Field	Simulation
49	30	681803.33	1494009.58	681802.90	1494007.53	9.47	9.48	7.86	7.91	27.48	25.75555
50	31.1	681796.85	1493982.25	-	-	5.00	-	5.81	-	14.57	
51	31.2	681794.70	1493984.11	681794.87	1493983.75	7.59	6.00	6.55	5.83	17.77	15.99991

Appendix C

The rewritten how to derive trunk diameter function

$Case1: y = ax^b$

Volume of a Mangrove Tree V

$V = 0.0687 \times 10^{0.724} \times (DBH^2 \cdot H)^{0.931}$

H(m): Tree height(m)

DBH(m): Diameter at breast height

BH: Breast height =1.3m

α:0.931

$V = \pi C(DBH^2 H)^{\alpha}$

C: 0.115826215

What to obtain is tree trunk shape radius r(h)

h: height from ground

$$\begin{cases} V = \int_0^H \pi r^2(h)dh = \pi C(DBH^2 H)^{\alpha} \\ 2 \cdot r(BH) = DBH \end{cases}$$

Obtain the function r(h)

$x = H - h$

h: distance from the tree top to down

$R(x) = r(H - h)$

Assumption of the function R(x)

$R(x) = ax^b$

$$r(BH) = R(H - BH) = \frac{DBH}{2}$$

$$\int_0^H \pi r^2(h)dh = \int_0^H \pi R^2(x)dx = \pi C \cdot DBH^{2\alpha} H^{\alpha}$$

$$\pi \int_0^H a^2 x^{2b} dx = \pi C \cdot DBH^{2\alpha} H^{\alpha}$$

$$\pi \left[\frac{a^2}{2b+1} x^{2b+1} \right]_0^H = \pi \frac{a^2}{2b+1} H^{2b+1} = \pi C \cdot DBH^{2\alpha} H^{\alpha}$$

$$\frac{a^2}{2b+1} H^{2b+1} = C \cdot DBH^{2\alpha} H^{\alpha}$$

$$\frac{a^2}{2b+1} H^{2b} = C \cdot DBH^{2\alpha} H^{\alpha-1}$$

$$\begin{cases} \frac{a^2}{2b+1} H^{2b} = C \cdot DBH^{2\alpha} H^{\alpha-1} \\ a(H - BH)^b = \frac{DBH}{2} \end{cases}$$

$$a = \frac{DBH}{2}(H - BH)^{-b}$$

$$\frac{\frac{DBH^2}{4}(H - BH)^{-2b}}{2b+1} H^{2b} = C \cdot DBH^{2\alpha} H^{\alpha-1}$$

$$\frac{(H - BH)^{-2b} H^{2b}}{2b+1} = 4 \cdot C \cdot DBH^{2(\alpha-1)} H^{\alpha-1}$$

$$\frac{\left(\frac{H}{H - BH}\right)^{2b}}{2b+1} = 4 \cdot C \cdot (DBH^2 H)^{\alpha-1}$$

$$\frac{c_1^{2b}}{2b+1} - c_2 = 0$$

$$c_1 = \frac{H}{H - BH}$$

$$c_2 = 4 \cdot C \cdot (DBH^2 H)^{\alpha-1}$$

Find b which fullfill this equation by iteration

*Case*2 : Cylinder from ground to BH, then $y = ax^b$

Volume of a Mangrove Tree V

$V = 0.0687 \times 10^{0.724} \times (DBH^2 \cdot H)^{0.931}$

H(m): Tree height(m)

DBH(m): Diameter at breast height

BH: Breast height =1.3m

α:0.931

$V = \pi C(DBH^2 H)^{\alpha}$

C: 0.115826215

What to obtain is tree trunk shape radius r(h)

h: height from ground

$$\begin{cases} V = \int_{BH}^{H} \pi r^2(h)dh + \pi DBH^2 BH = \pi C(DBH^2 H)^{\alpha} \\ 2 \cdot r(BH) = DBH \end{cases}$$

Obtain the function r(h)

$x = H - h$

h: distance from the tree top to down

$R(x) = r(H - h)$

Assumption of the function R(x)

$R(x) = ax^b$

$$r(BH) = R(H - BH) = \frac{DBH}{2}$$

$$\int_{BH}^{H} \pi r^2(h)dh = \int_{0}^{H-BH} \pi R^2(x)dx = \pi C \cdot DBH^{2\alpha} H^{\alpha} - \pi \frac{DBH^2}{4} BH$$

$$\pi \int_{0}^{H-VH} a^2 x^{2b} dx = \pi C \cdot DBH^{2\alpha} H^{\alpha} - \pi \frac{DBH^2}{4} BH$$

$$\pi \left[\frac{a^2}{2b+1} x^{2b+1} \right]_{0}^{H-BH} = \pi \frac{a^2}{2b+1} (H - BH)^{2b+1} = \pi C \cdot DBH^{2\alpha} H^{\alpha} - \pi \frac{DBH^2}{4} BH$$

$$\frac{a^2}{2b+1} (H - BH)^{2b+1} = C \cdot DBH^{2\alpha} H^{\alpha} - \frac{DBH^2}{4} BH$$

$$\frac{a^2}{2b+1} (H - BH)^{2b} = \frac{C \cdot DBH^{2\alpha} H^{\alpha} - \frac{DBH^2}{4} BH}{H - BH}$$

$$\begin{cases} \frac{a^2}{2b+1} (H - BH)^{2b} = \frac{C \cdot DBH^{2\alpha} H^{\alpha} - \frac{DBH^2}{4} BH}{H - BH} \\ a(H - BH)^b = \frac{DBH}{2} \end{cases}$$

$$a = \frac{DBH}{2}(H - BH)^{-b}$$

$$\frac{\frac{DBH^2}{4}(H-BH)^{-2b}}{2b+1}(H-BH)^{2b} = \frac{C \cdot DBH^{2\alpha} H^{\alpha} - \frac{DBH^2}{4} BH}{H - BH}$$

$$\frac{\frac{DBH^2}{4}}{2b+1} = \frac{C \cdot DBH^{2\alpha} H^{\alpha} - \frac{DBH^2}{4} BH}{H - BH}$$

$$2b+1 = \frac{H - BH}{C \cdot DBH^{2\alpha} H^{\alpha} - \frac{DBH^2}{4} BH} \frac{DBH^2}{4}$$

$$b = \frac{1}{2}\left(\frac{(H-BH)DBH^2}{4C \cdot DBH^{2\alpha} H^{\alpha} - DBH^2 BH} - 1\right) = \frac{1}{2}\left(\frac{H - BH}{4C \cdot DBH^{2(\alpha-1)} H^{\alpha} - BH} - 1\right)$$

Volume of a Mangrove under Water (depth =d)

if d $\leq$ 1.3m

$$V_{h<d} = \pi \frac{DBH^2}{4} d$$

if d $\geq$1.3m

$$V_{h<d} = \pi \frac{DBH^2}{4} 1.3 + \pi \left[\frac{a^2}{2b+1} x^{2b+1}\right]_{H-d}^{H-1.3} = \pi \frac{DBH^2}{4} 1.3 + \pi \frac{a^2}{2b+1}((H-1.3)^{2b+1} - (H-d)^{2b+1})$$

Proejcted Area of a Mangrove under Water (depth =d)

if d $\leq$ 1.3m

$$A_{h<d} = DBH \cdot d$$

if d $\geq$1.3m

$$A_{h<d} = DBH \cdot d + \int_{1.3}^{d} 2r(h)dh = DBH \cdot d + \int_{H-d}^{H-1.3} 2R(x)dx = DBH \cdot d + \int_{H-d}^{H-1.3} 2ax^b dx$$

$$= DBH \cdot d + \left[\frac{2a}{b+1} x^{b+1}\right]_{H-d}^{H-1.3} = DBH \cdot d + \frac{2a}{b+1}((H-1.3)^{b+1} - (H-d)^{b+1})$$

Case 3. Chopped Cone

Volume of a Mangrove Tree V

$V = 0.0687 \times 10^{0.724} \times (DBH^2 \cdot H)^{0.931}$

H(m): Tree height(m)

DBH(m): Diameter at breast height

BH: Breast height =1.3m

α:0.931

$V = \pi C (DBH^2 H)^{\alpha}$

C: 0.115826215

What to obtain is tree trunk shape radius r(h)

h: height from ground

$$\begin{cases} V = \int_0^H \pi r^2(h)dh = \pi C(DBH^2 H)^{\alpha} \\ 2 \cdot r(BH) = DBH \end{cases}$$

Obtain the function r(h)

Assumption of the function r(h): Chopped Cone

$$r_{con}(h) = \frac{DBH/2 - D0/2}{BH} h + D0/2$$

$$= \frac{DBH - D_0}{2BH} h + \frac{D_0}{2} = a_{con} h + b_{con}$$

$$a_{con} = \frac{DBH - D_0}{2BH}$$

$$b_{con} = \frac{D_0}{2}$$

$$V = \int_0^H \pi r_{con}{}^2(h)dh = \pi C \cdot DBH^{2\alpha} H^{\alpha}$$

$$\pi \int_0^H \left(a_{con} h + b_{con}\right)^2 dh = \pi C \cdot DBH^{2\alpha} H^{\alpha}$$

$$\pi \left[\frac{a_{con}{}^2}{3} h^3 + a_{con} b_{con} h^2 + b_{con}{}^2 h \right]_0^H = \pi \left(\frac{a_{con}{}^2}{3} H^3 + a_{con} b_{con} H^2 + b_{con}{}^2 H \right) = \pi C \cdot DBH^{2\alpha} H^{\alpha}$$

$$\frac{DBH^2 - 2 \cdot DBH \cdot D_0 + D_0{}^2}{12BH^2} H^3 + \frac{DBH \cdot D_0 - D_0{}^2}{4BH} H^2 + \frac{D_0{}^2}{4} H = C \cdot DBH^{2\alpha} H^{\alpha}$$

$$\left(\frac{H^3}{12BH^2} - \frac{H^2}{4BH} + \frac{H}{4}\right) D_0{}^2 + \left(\frac{-DBH}{6BH^2} H^3 + \frac{DBH \cdot}{4BH} H^2\right) D_0 + \frac{DBH^2}{12BH^2} H^3 - C \cdot DBH^{2\alpha} H^{\alpha} = 0$$

$$(2b+1)\log(\frac{H}{H-BH})-\log(2b+1)=\log(4\cdot C\cdot(DBH^2H)^{\alpha-1}\frac{H}{H-BH})$$

$$B=2b+1$$

$$c_3\cdot B-\log B=c_4$$

$$c_3=\log(\frac{H}{H-BH})$$

$$c_4=\log(4\cdot C\cdot(DBH^2H)^{\alpha-1}\frac{H}{H-BH})$$

$$c_3\cdot B-\log B-c_4=0$$

$$g(B)=c_3\cdot B-\log B-c_4$$

$$g'(B)=c_3-B^{-1}$$

$$g''(B)=1+B^{-2}$$

$$g'''(B)=-2B^{-3}$$

$$c_3\cdot B-c_4=\log B$$

$$B-e^{c_3\cdot B-c_4}=0$$

$$f(B)=B-e^{c_3\cdot B-c_4}$$

$$f'(B)=1-c_3(c_3\cdot B-c_4)$$

$$f''(B)=-{c_3}^2$$

Appendix D

The table of volume calculation for every 0.5m from 0m to 5m

T_ID	H	DBH	Vs*	a	b	V(0.5)	V(1.0)	V(1.5)	V(2.0)	V(2.5)	V(3.0)	V(3.5)	V(4.0)	V(4.5)	V(5.0)	V(H)**
1.1	8.01	0.22	0.1483	0.02576	0.75826	0.0187	0.0374	0.0559	0.0727	0.0876	0.1005	0.1116	0.1210	0.1288	0.1350	0.1483
1.2	8.16	0.26	0.2058	0.02775	0.79746	0.0261	0.0522	0.0780	0.1015	0.1221	0.1399	0.1552	0.1681	0.1788	0.1874	0.2058
1.3	8.25	0.33	0.3251	0.03090	0.86046	0.0422	0.0844	0.1261	0.1637	0.1965	0.2247	0.2486	0.2686	0.2849	0.2979	0.3251
1.4	7.44	0.19	0.1111	0.02503	0.74601	0.0148	0.0295	0.0441	0.0573	0.0688	0.0787	0.0870	0.0939	0.0995	0.1038	0.1111
2	9.23	0.31	0.3197	0.02846	0.81401	0.0370	0.0741	0.1108	0.1445	0.1745	0.2012	0.2246	0.2449	0.2623	0.2769	0.3197
3	7.16	0.21	0.1237	0.02647	0.77751	0.0172	0.0344	0.0514	0.0666	0.0797	0.0908	0.0999	0.1074	0.1132	0.1175	0.1237
4	6.79	0.21	0.1161	0.02695	0.79252	0.0170	0.0339	0.0507	0.0655	0.0780	0.0885	0.0969	0.1036	0.1086	0.1121	0.1161
6	5.39	0.17	0.0619	0.02615	0.82134	0.0109	0.0217	0.0324	0.0414	0.0484	0.0537	0.0575	0.0599	0.0613	0.0618	0.0619
7	8.50	0.28	0.2441	0.02819	0.80608	0.0301	0.0602	0.0900	0.1171	0.1411	0.1620	0.1801	0.1955	0.2084	0.2189	0.2441
8.1	6.86	0.20	0.1091	0.02631	0.77817	0.0157	0.0314	0.0469	0.0607	0.0724	0.0823	0.0903	0.0966	0.1015	0.1050	0.1091
8.2	6.82	0.21	0.1217	0.02721	0.79762	0.0178	0.0355	0.0531	0.0686	0.0817	0.0926	0.1015	0.1085	0.1137	0.1174	0.1217
8.3	7.29	0.19	0.1086	0.02522	0.75100	0.0147	0.0294	0.0440	0.0570	0.0684	0.0781	0.0862	0.0929	0.0982	0.1023	0.1086
8.4	6.53	0.18	0.0825	0.02513	0.75905	0.0122	0.0244	0.0365	0.0472	0.0562	0.0637	0.0697	0.0744	0.0779	0.0803	0.0825
8.5	6.18	0.16	0.0666	0.02449	0.75297	0.0102	0.0205	0.0306	0.0395	0.0469	0.0529	0.0577	0.0613	0.0638	0.0654	0.0666
9.1	6.79	0.20	0.1084	0.02644	0.78191	0.0157	0.0315	0.0471	0.0608	0.0725	0.0823	0.0902	0.0965	0.1012	0.1046	0.1084
9.2	5.76	0.16	0.0604	0.02491	0.77534	0.0099	0.0198	0.0296	0.0380	0.0448	0.0502	0.0543	0.0572	0.0590	0.0600	0.0604
10	5.43	0.17	0.0628	0.02614	0.81886	0.0109	0.0219	0.0327	0.0417	0.0489	0.0543	0.0581	0.0607	0.0621	0.0627	0.0628
11.1	6.56	0.20	0.1040	0.02673	0.79243	0.0156	0.0312	0.0466	0.0601	0.0715	0.0809	0.0883	0.0941	0.0984	0.1013	0.1040
11.3	6.16	0.15	0.0560	0.02332	0.72826	0.0085	0.0171	0.0255	0.0330	0.0392	0.0443	0.0483	0.0514	0.0536	0.0550	0.0560
12	4.54	0.13	0.0353	0.02469	0.84944	0.0071	0.0141	0.0210	0.0265	0.0304	0.0330	0.0345	0.0352	0.0353	0.0353	0.0353
13	8.31	0.31	0.2945	0.03002	0.84245	0.0377	0.0753	0.1126	0.1463	0.1757	0.2012	0.2230	0.2412	0.2563	0.2683	0.2945
14.1	9.70	0.34	0.3972	0.02895	0.82704	0.0445	0.0890	0.1331	0.1737	0.2102	0.2427	0.2715	0.2966	0.3184	0.3369	0.3972
14.2	7.11	0.24	0.1530	0.02816	0.81296	0.0218	0.0436	0.0651	0.0842	0.1005	0.1142	0.1254	0.1343	0.1412	0.1463	0.1530
15	8.35	0.26	0.2152	0.02763	0.79489	0.0267	0.0535	0.0800	0.1041	0.1253	0.1439	0.1599	0.1735	0.1848	0.1940	0.2152
16	9.15	0.33	0.3728	0.02973	0.83883	0.0440	0.0881	0.1318	0.1717	0.2071	0.2384	0.2657	0.2892	0.3092	0.3259	0.3728
17	6.57	0.20	0.1001	0.02643	0.78576	0.0149	0.0299	0.0447	0.0577	0.0686	0.0776	0.0849	0.0905	0.0946	0.0974	0.1001
18	9.36	0.30	0.3106	0.02797	0.80519	0.0354	0.0708	0.1059	0.1382	0.1671	0.1929	0.2155	0.2353	0.2523	0.2667	0.3106
20.1	10.02	0.30	0.3352	0.02711	0.79354	0.0359	0.0718	0.1074	0.1404	0.1703	0.1972	0.2212	0.2425	0.2611	0.2773	0.3352
20.2	9.91	0.36	0.4677	0.02963	0.84248	0.0519	0.1038	0.1553	0.2027	0.2453	0.2833	0.3170	0.3465	0.3721	0.3940	0.4677

21	7.54	0.22	0.1437	0.02663	0.77744	0.0192	0.0384	0.0574	0.0745	0.0893	0.1021	0.1128	0.1216	0.1287	0.1342	0.1437
22.1	5.42	0.17	0.0656	0.02649	0.82805	0.0115	0.0230	0.0343	0.0438	0.0513	0.0569	0.0609	0.0635	0.0649	0.0655	0.0656
22.2	4.67	0.11	0.0266	0.02227	0.77016	0.0051	0.0101	0.0151	0.0192	0.0222	0.0243	0.0257	0.0264	0.0266	0.0266	0.0266
22.3	4.37	0.15	0.0431	0.02672	0.93254	0.0091	0.0182	0.0270	0.0338	0.0384	0.0412	0.0426	0.0430	0.0431	0.0431	0.0431
23	6.68	0.21	0.1125	0.02700	0.79561	0.0167	0.0333	0.0498	0.0643	0.0765	0.0866	0.0948	0.1011	0.1058	0.1091	0.1125
24	7.94	0.24	0.1704	0.02690	0.78112	0.0219	0.0438	0.0655	0.0851	0.1023	0.1172	0.1299	0.1406	0.1493	0.1563	0.1704
25	9.31	0.30	0.3006	0.02785	0.80251	0.0344	0.0687	0.1028	0.1341	0.1622	0.1871	0.2091	0.2282	0.2447	0.2586	0.3006
26.1	8.86	0.23	0.1811	0.02530	0.75054	0.0210	0.0419	0.0627	0.0818	0.0989	0.1142	0.1275	0.1392	0.1492	0.1576	0.1811
26.2	8.34	0.23	0.1716	0.02605	0.76378	0.0210	0.0420	0.0628	0.0818	0.0987	0.1134	0.1262	0.1372	0.1463	0.1538	0.1716
27.1	10.27	0.28	0.3057	0.02600	0.77415	0.0317	0.0634	0.0949	0.1242	0.1509	0.1750	0.1967	0.2161	0.2332	0.2481	0.3057
27.2	9.98	0.26	0.2612	0.02552	0.76205	0.0276	0.0551	0.0825	0.1079	0.1310	0.1518	0.1705	0.1872	0.2018	0.2145	0.2612
28.1	8.37	0.22	0.1596	0.02548	0.75263	0.0194	0.0387	0.0579	0.0755	0.0910	0.1048	0.1167	0.1269	0.1355	0.1425	0.1596
28.2	8.44	0.25	0.1945	0.02670	0.77681	0.0237	0.0475	0.0710	0.0925	0.1115	0.1282	0.1427	0.1551	0.1654	0.1740	0.1945
28.3	7.78	0.23	0.1636	0.02699	0.78344	0.0214	0.0428	0.0640	0.0831	0.0998	0.1142	0.1264	0.1366	0.1448	0.1513	0.1636
28.4	6.56	0.21	0.1129	0.02734	0.80544	0.0170	0.0341	0.0509	0.0656	0.0780	0.0881	0.0962	0.1024	0.1070	0.1100	0.1129
29	8.53	0.31	0.2961	0.02952	0.83254	0.0369	0.0738	0.1103	0.1435	0.1727	0.1981	0.2200	0.2385	0.2539	0.2664	0.2961
30	7.91	0.26	0.1996	0.02813	0.80555	0.0260	0.0521	0.0779	0.1012	0.1214	0.1389	0.1538	0.1661	0.1762	0.1841	0.1996
31.2	5.83	0.16	0.0619	0.02490	0.77255	0.0101	0.0201	0.0300	0.0386	0.0456	0.0511	0.0553	0.0584	0.0603	0.0614	0.0619
	353.13	**10.80**	**8.1878**			**1.0386**	**2.0772**	**3.1057**	**4.0327**	**4.8416**	**5.5392**	**6.1326**	**6.6292**	**7.0370**	**7.3645**	**8.1878**

Vs* : tree trunk volume calculated by Komiyama' model
V(H)**: tree trunk volume calculated by Integration

Appendix E

The projected area of 0.5m interval from 0m to 5m.

T_ID	H	DBH	a	b	A(0.5)	A(1.0)	A(1.5)	A(2.0)	A(2.5)	A(3.0)	A(3.5)	A(4.0)	A(4.5)	A(5.0)	A(H)*
1.1	8.01	0.22	0.02576	0.75826	0.109	0.218	0.314	0.386	0.454	0.517	0.576	0.630	0.679	0.723	0.865
1.2	8.16	0.26	0.02775	0.79746	0.129	0.258	0.370	0.455	0.534	0.608	0.677	0.739	0.796	0.847	1.017
1.3	8.25	0.33	0.03090	0.86046	0.164	0.328	0.470	0.576	0.675	0.766	0.851	0.928	0.998	1.060	1.263
1.4	7.44	0.19	0.02503	0.74601	0.097	0.194	0.279	0.343	0.403	0.458	0.509	0.556	0.598	0.634	0.730
2	9.23	0.31	0.02846	0.81401	0.154	0.307	0.441	0.542	0.638	0.728	0.812	0.890	0.963	1.029	1.326
3	7.16	0.21	0.02647	0.77751	0.105	0.209	0.301	0.369	0.433	0.491	0.544	0.592	0.634	0.671	0.752
4	6.79	0.21	0.02695	0.79252	0.104	0.208	0.299	0.366	0.428	0.484	0.535	0.580	0.619	0.652	0.711
6	5.39	0.17	0.02615	0.82134	0.083	0.166	0.239	0.291	0.337	0.377	0.410	0.438	0.458	0.470	0.474
7	8.50	0.28	0.02819	0.80608	0.138	0.277	0.398	0.489	0.574	0.654	0.728	0.796	0.859	0.915	1.123
8.1	6.86	0.20	0.02631	0.77817	0.100	0.200	0.287	0.353	0.413	0.468	0.517	0.562	0.600	0.633	0.695
8.2	6.82	0.21	0.02721	0.79762	0.106	0.213	0.305	0.374	0.438	0.495	0.547	0.593	0.633	0.667	0.729
8.3	7.29	0.19	0.02522	0.75100	0.097	0.193	0.278	0.342	0.402	0.457	0.507	0.553	0.593	0.629	0.715
8.4	6.53	0.18	0.02513	0.75905	0.088	0.176	0.254	0.311	0.364	0.412	0.455	0.494	0.526	0.554	0.596
8.5	6.18	0.16	0.02449	0.75297	0.081	0.162	0.232	0.285	0.333	0.376	0.415	0.448	0.476	0.498	0.525
9.1	6.79	0.20	0.02644	0.78191	0.100	0.200	0.288	0.353	0.413	0.468	0.517	0.561	0.599	0.631	0.689
9.2	5.76	0.16	0.02491	0.77534	0.079	0.159	0.228	0.279	0.325	0.366	0.401	0.431	0.455	0.472	0.484
10	5.43	0.17	0.02614	0.81886	0.083	0.167	0.240	0.292	0.338	0.379	0.413	0.441	0.461	0.474	0.479
11.1	6.56	0.20	0.02673	0.79243	0.100	0.199	0.286	0.351	0.410	0.463	0.511	0.553	0.589	0.619	0.665
11.3	6.16	0.15	0.02332	0.72826	0.074	0.148	0.212	0.261	0.305	0.345	0.381	0.412	0.438	0.459	0.484
12	4.54	0.13	0.02469	0.84944	0.067	0.134	0.192	0.233	0.267	0.295	0.316	0.329	0.335	0.335	0.335
13	8.31	0.31	0.03002	0.84245	0.155	0.310	0.445	0.545	0.639	0.726	0.807	0.881	0.948	1.008	1.211
14.1	9.70	0.34	0.02895	0.82704	0.168	0.337	0.483	0.594	0.699	0.798	0.891	0.978	1.059	1.134	1.503
14.2	7.11	0.24	0.02816	0.81296	0.118	0.235	0.338	0.414	0.485	0.549	0.607	0.659	0.705	0.744	0.827
15	8.35	0.26	0.02763	0.79489	0.130	0.261	0.375	0.461	0.541	0.617	0.687	0.751	0.810	0.863	1.050
16	9.15	0.33	0.02973	0.83883	0.167	0.335	0.481	0.590	0.694	0.790	0.881	0.965	1.042	1.113	1.417
17	6.57	0.20	0.02643	0.78576	0.098	0.195	0.280	0.343	0.401	0.454	0.501	0.543	0.578	0.607	0.653
18	9.36	0.30	0.02797	0.80519	0.150	0.300	0.431	0.531	0.624	0.713	0.796	0.873	0.945	1.012	1.317
20.1	10.02	0.30	0.02711	0.79354	0.151	0.302	0.435	0.535	0.631	0.721	0.807	0.888	0.963	1.033	1.412
20.2	9.91	0.36	0.02963	0.84248	0.182	0.363	0.522	0.641	0.754	0.861	0.961	1.055	1.143	1.224	1.638

21	7.54	0.22	0.02663	0.77744	0.111	0.221	0.318	0.390	0.458	0.521	0.578	0.630	0.677	0.718	0.827
22.1	5.42	0.17	0.02649	0.82805	0.086	0.171	0.246	0.299	0.346	0.388	0.422	0.450	0.471	0.484	0.488
22.2	4.67	0.11	0.02227	0.77016	0.057	0.114	0.163	0.198	0.229	0.255	0.275	0.290	0.297	0.298	0.298
22.3	4.37	0.15	0.02672	0.93254	0.076	0.152	0.218	0.262	0.298	0.326	0.346	0.358	0.361	0.361	0.361
23	6.68	0.21	0.02700	0.79561	0.103	0.206	0.296	0.362	0.424	0.479	0.529	0.573	0.611	0.642	0.695
24	7.94	0.24	0.02690	0.78112	0.118	0.236	0.339	0.417	0.490	0.557	0.620	0.677	0.729	0.775	0.919
25	9.31	0.30	0.02785	0.80251	0.148	0.296	0.425	0.523	0.615	0.702	0.784	0.861	0.931	0.996	1.294
26.1	8.86	0.23	0.02530	0.75054	0.115	0.231	0.332	0.409	0.483	0.551	0.616	0.676	0.732	0.783	0.998
26.2	8.34	0.23	0.02605	0.76378	0.116	0.231	0.333	0.409	0.482	0.549	0.612	0.670	0.724	0.772	0.945
27.1	10.27	0.28	0.02600	0.77415	0.142	0.284	0.409	0.504	0.594	0.681	0.763	0.840	0.912	0.980	1.370
27.2	9.98	0.26	0.02552	0.76205	0.132	0.265	0.381	0.470	0.554	0.635	0.711	0.783	0.850	0.913	1.255
28.1	8.37	0.22	0.02548	0.75263	0.111	0.222	0.319	0.393	0.463	0.528	0.589	0.646	0.697	0.744	0.915
28.2	8.44	0.25	0.02670	0.77681	0.123	0.246	0.354	0.435	0.511	0.583	0.650	0.712	0.768	0.819	1.007
28.3	7.78	0.23	0.02699	0.78344	0.117	0.233	0.335	0.412	0.484	0.550	0.611	0.667	0.718	0.762	0.893
28.4	6.56	0.21	0.02734	0.80544	0.104	0.208	0.299	0.366	0.427	0.483	0.533	0.576	0.613	0.644	0.690
29	8.53	0.31	0.02952	0.83254	0.153	0.306	0.440	0.540	0.634	0.721	0.802	0.877	0.945	1.006	1.230
30	7.91	0.26	0.02813	0.80555	0.129	0.258	0.370	0.454	0.533	0.606	0.673	0.734	0.789	0.839	0.987
31.2	5.83	0.16	0.02490	0.77255	0.080	0.160	0.230	0.281	0.328	0.369	0.405	0.436	0.460	0.479	0.493
	353.13	**10.80**			**5.398**	**10.795**	**15.510**	**19.030**	**22.302**	**25.321**	**28.081**	**30.574**	**32.791**	**34.729**	**41.349**

A(H)**: projected area calculated by Integration

Appendix F
Field Photo

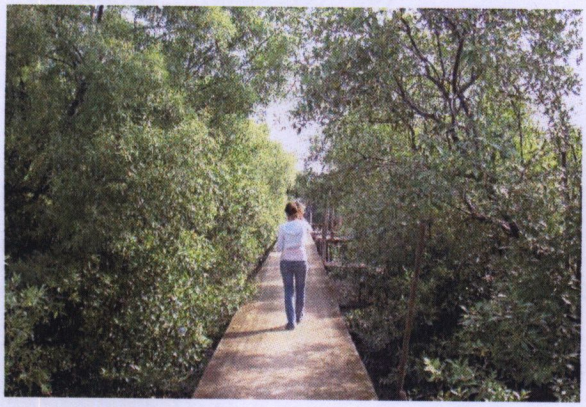

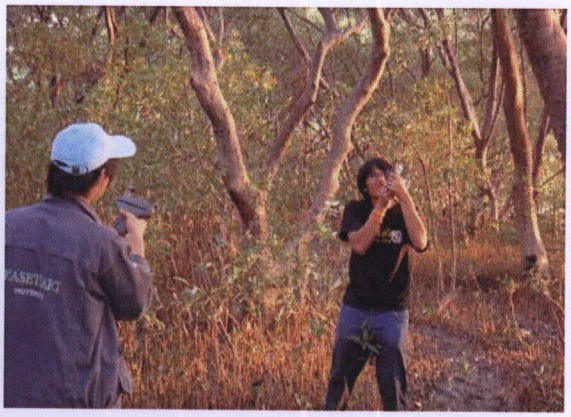

Appendix G

Mangrove Shape algorithm in C program

```
#include<stdio.h>
#include<math.h>
#include<malloc.h>
#include<stdlib.h>

/*
        This program creates a tree that follows Komiyama Mangrove Tree Volume model.
        Authored by K.Honda AIT    30 April 2009

        This program finds R(x)=a*x^b, R(x) Radius of the trunk, x: disatance from top to
down
        which fullfill two conditions
                (a) Volume from R(x): Integral of pai*R(x)^2, [0,H] = Komiyama model(
volumeKomiyama( H, DBH ) )
                (b) R(H-BH) = DBH
                                H: Tree height, BH: Breast Height 1.3m

        The searching range of b is [BMIN, BMAX]=[0,2.5],
        assuming the only one solution exist within this range.
        It is possible that there is no solution accroding to the combinatino of H and DBH
*/

//#define       PAI     M_PI
#definePAI      (atan(1.0)*4.0)

// Iteration criteria
#defineEPS      (1.0E-7)

// Breast Height = 1.3m
#defineBH       1.3

// VERBOSE Switch to output iteration process
#defineVERBOSE      1

/*
        define Komiyama model

        Volume          = 0.0687/1000*(DBH(cm)^2*H)^0.931 ( DBH in cm )
                        = 0.0687/1000*10000^alpha*(DBH^2*H)^0.931
                        = 0.0687*power(10,0.724)*(DBH^2*H)^0.931
                        = pai * C * ( DBH^2 * H ) ^ alpha
                        alpha = 0.931
                        C: 0.115826215
        Note; original Komiyama model's DBH is in centi-meter while H is in meter
*/
```

```
#definealpha  0.931
#defineC      (0.0687/1000/PAI*pow(10000.,alpha))

/* BMIN, BMAX: Search range of parameter b */
#defineBMIN 0
#defineBMAX       2.5

#defineMAX_ITERATION  100

/*      shape is represented by radius R(x)=a*x^b
        R(x): Radius, where x is from top to down
        r(h): Rdaius, where h is height from the ground.
        R(x) = r(H-h), x = H-h: H is tree height.

        h=[0,BH] Cylinder with Diameter DBH
        h=[BH,H] R(x)=a*x^b, x=H-h, x[0,H-h]
*/
typedef struct ST_SHAPE_AXB
{
        int             valid;
        double a;
        double b;
} SHAPE_AXB;

/*      shape is represented by chopped cone
        R(x): Radius, where x is from top to down
        r(h): Rdaius, where h is height from the ground.
        R(x) = r(H-h), x = H-h: H is tree height.
*/
typedef struct ST_SHAPE_CONE
{
        int             valid;
        double DBH;
        double D0;
} SHAPE_CONE;


typedef struct ST_TREE
{
        int     id;
        double H;
        double dbh;
        double volume;
        SHAPE_AXB axb;
        SHAPE_CONE      cone;
} TREE;


TREE *newTree( int id, double H, double DBH );
int komiyamaShapeAxb( double H, double DBH, double *a, double *b, int verbose );
```

```
double evaluate( double b, double c1, double c2 );
printTree( TREE *tree );
double volumeKomiyama( double H, double DBH );
double volumeIntegration( double H, double a, double b );
double R( double x, double a, double b );
int komiyamaShapeAxbCylinder( double H, double DBH, double *a, double *b, int
verbose );
int komiyamaShapeCone( double H, double DBH, double *D0, int verbose );
double findConeD0( double H, double DBH );
double volumeCone( double H, double DBH, double D0 );
double rcone(double h, double DBH, double D0);

usage()
{
        fprintf(stderr, "usage: mangroveShape H DBH\n");
}

int     main( int argc, char **argv )
{
        TREE  *tree;
        double H=10.0, DBH=0.1;
        int     id=1;

        if( argc != 3 ){
                usage();
                exit(1);
        }

        H = atof( argv[1] );
        DBH = atof( argv[2] );

        tree = newTree( id, H, DBH );
        printTree( tree );
}


printTree( TREE *tree )
{
        printf("tree id:%5d
H:%.2lf\tDBH:%.2lf\tVolume:%.3lf\taxbValid:%d\ta:%.7lf\tb:%.5lf\n",
                tree->id, tree->H, tree->dbh, tree->volume, tree->axb.valid, tree->axb.a,
tree->axb.b);
}

// create a tree
TREE *newTree( int id, double H, double DBH )
{
        TREE *tree;
        double a, b;
//      double D0;
```

```
        tree = malloc( sizeof( TREE ) );

        tree->id = id;
        tree->H = H;
        tree->dbh = DBH;
//      tree->axb.valid = komiyamaShapeAxb( H, DBH, &a, &b, VERBOSE );
//      tree->axb.a = a;
//      tree->axb.b = b;
        tree->axb.valid = komiyamaShapeAxbCylinder( H, DBH, &a, &b, VERBOSE );
        tree->axb.a = a;
        tree->axb.b = b;
//      tree->cone.valid = komiyamaShapeCone( H, DBH, &D0, VERBOSE );
//      tree->cone.DBH = DBH;
//      tree->cone.D0 = D0;
        tree->volume = volumeKomiyama( H, DBH );
//      printf("newTree: H:%lf DBH:%lf a:%lf b:%lf vol:%lf\n", H, DBH, a, b, tree-
>volume);
        return tree;
}

/*
        Find a function R(x) = a * x^b (R:radius, x: distance from the top )
        by simple iteration
*/
int komiyamaShapeAxb( double H, double DBH, double *a, double *b, int verbose )
{
        double c1, c2;
        double b1, b2, bc;
        double e1, e2, ec;
        int     iteration=0;

        double vKomiyama, vab;
        double DBHab;

        c1 = H/(H-BH);
        c2 = 4. * C * pow(DBH*DBH*H, alpha-1);

        b1 = BMIN;
        b2 = BMAX;
        e1 = evaluate( b1, c1, c2 );
        e2 = evaluate( b2, c1, c2 );

        if( verbose ){
                printf("komiyamaShapeAxb: EPS = %lg\n", EPS );
                printf("komiyamaShapeAxb: H:%lf\tBH:%lf\talpha:%lf\tC:%lf\n",
                        H, BH, alpha, C );
                printf("komiyamaShapeAxb: c1=H/(H-
BH):%lf\tc2=4C(DBH^2*H)^alpha):%lf\n",
                        c1, c2 );
```

```
        }
        if( e1*e2 > 0 ){
                int     nstep = 1000;
                int     i, found = 0;
                double db;

                db = (BMAX-BMIN)/nstep;
                for(b1=BMIN,i=0;i<nstep;i++, b1+=db){
                        b2=b1+db;
                        e1 = evaluate( b1, c1, c2 );
                        e2 = evaluate( b2, c1, c2 );
                        if( e1*e2 <=0 ) {
                                found = 1;
                                break;
                        }
                }
                if( ! found ){
                        fprintf(stderr, "cannot obatain the solution %lf %lf\n", e1, e2);
                        fprintf(stderr, "Volume by Komiyama: %lf\n",volumeKomiyama(
H, DBH ) );
                        fprintf(stderr, "Volume by Cyliner: %lf\n",
PAI*(DBH/2)*(DBH/2)*H    );
                        fprintf(stderr, "Volume by Cone   : %lf\n",
PAI*(DBH/2)*(DBH/2)*H/3. );
                        return 0;
                }
        }
        if( e2 < e1 ){
                double wk;
                wk = b1;        b1 = b2;        b2 = wk;
                wk = e1;        e1 = e2;        e2 = wk;
        }
        while( 1 ){
                iteration++;
                if( iteration > MAX_ITERATION ){
                        fprintf(stderr, "reatch to max iteration %d\n", iteration);
                        exit(1);
                }
                bc = (b1+b2)/2.;
                ec = evaluate( bc, c1, c2 );
                if(verbose){
                        printf("komiyamaShapeAxb: %d b:%lf ec( (c1^(2b))/(2b+1) - c2)
:%lf\n",
                                        iteration, bc, ec);
                }
                if( fabs(ec) < EPS ){
                        *b = bc;
                        break;
                }
                if( ec < 0 ){
```

```
                b1 = bc;
            } else {
                b2 = bc;
            }
        }
        *a = DBH/2.0*pow(H-BH, -1.0*(*b));

        vKomiyama = volumeKomiyama( H, DBH );
        vab = volumeIntegration( H, *a, *b );
        DBHab = 2.0*R(H-BH, *a, *b );
        if(verbose){
            printf("komiyamaShapeAxb: Volume by Komiyama %lf\tVolume by
integratinon %lf\n", vKomiyama, vab);
            printf("komiyamaShapeAxb: DBH given %lf\tDBH by R(H-h) %lf\n",
DBH, DBHab);
        }
        if( fabs(vKomiyama - vab) > EPS*100){
            fprintf(stderr, "komiyamaShapeAxb: volume incosistent:
VolKomiyama:%lf != Vol Integration:%lf\n",
                vKomiyama, vab );
        }
        if( fabs( DBH - DBHab ) > EPS*100 ){
            fprintf(stderr, "komiyamaShapeAxb: DBH incosistent: DBH:%lf != DBH
by r(h):%lf\n",
                DBH, DBHab);
        }
//      printf("komiyamaShapeAxb: H: %.2lf\tDBH:%.2lf\ta:%lf\tb:%lf\n",H,DBH,*a,*b);
        return 1;
}

double evaluate( double b, double c1, double c2 )
{
        return pow(c1, 2*b) / ( 2*b + 1 ) - c2;
}

// Calculate Komiyama Model H:Tree height in meter, DBH: Diameter at Breast Heigth in
meter
double volumeKomiyama( double H, double DBH )
{
        return 0.0687/1000.*pow((DBH*100)*(DBH*100)*H, 0.931);
}

// Calculate the Tree Volume from the intergral of R(x)=a*x^b
double volumeIntegration( double H, double a, double b )
{
            return PAI*a*a/(2*b+1)*pow(H, 2*b+1);

}

//      Function R
```

```
double R( double x, double a, double b )
{
        return a*pow(x,b);
}

int komiyamaShapeAxbCylinder( double H, double DBH, double *a, double *b, int
verbose )
{
        int     iteration=0;

        double vKomiyama, vab;
        double DBHab;

        *b = ((H-BH)/(4*C*pow(DBH,2*(alpha-1))*pow(H,alpha)-BH)-1)/2.;
        *a = DBH/2.0*pow(H-BH, -1.0*(*b));

        vKomiyama = volumeKomiyama( H, DBH );
        vab = volumeIntegration( H-BH, *a, *b )+PAI*BH*(DBH*DBH)/4;
        DBHab = 2.0*R(H-BH, *a, *b );
        if(verbose){
                printf("komiyamaShapeAxbCylinder: Volume by Komiyama %lf\tVolume
by integratinon %lf\n", vKomiyama, vab);
                printf("komiyamaShapeAxbCylinder: DBH given %lf\tDBH by R(H-h)
%lf\n", DBH, DBHab);
        }
        if( fabs(vKomiyama - vab) > EPS*100){
                fprintf(stderr, "komiyamaShapeAxbCylinder: volume incosistent:
VolKomiyama:%lf != Vol Integration:%lf\n",
                        vKomiyama, vab );
        }
        if( fabs( DBH - DBHab ) > EPS*100 ){
                fprintf(stderr, "komiyamaShapeAxbCylinder: DBH incosistent: DBH:%lf
!= DBH by r(h):%lf\n",
                        DBH, DBHab);
        }
        printf("komiyamaShapeAxbCylinder: H:
%.2lf\tDBH:%.2lf\ta:%lf\tb:%lf\n",H,DBH,*a,*b);
        return 1;
}

int komiyamaShapeCone( double H, double DBH, double *D0, int verbose )
{
        double vKomiyama, vcone, DBHcone, rH;

        *D0 = findConeD0( H, DBH );

        printf("komiyamaShapeCone: D0:%lf\n", *D0);
        vKomiyama = volumeKomiyama( H, DBH );
        vcone = volumeCone( H, DBH, *D0 );
        DBHcone = 2.0*rcone(BH, DBH, *D0 );
```

```
	rH = rcone(H, DBH, *D0 );
	printf("komiyamaShapeCone: D0:%lf, Diameter at the top %lf \n", *D0, rH*2.);
	if(verbose){
		printf("komiyamaShapeCone: Volume by Komiyama %lf\tVolume by
integratinon %lf\n", vKomiyama, vcone);
		printf("komiyamaShapeCone: DBH given %lf\tDBH by R(H-h) %lf\n",
DBH, DBHcone);
	}
	if( fabs(vKomiyama - vcone) > EPS*100){
		fprintf(stderr, "komiyamaShapeCone: volume incosistent:
VolKomiyama:%lf != Vol Integration:%lf\n",
			vKomiyama, vcone );
	}
	if( fabs( DBH - DBHcone ) > EPS*100 ){
		fprintf(stderr, "komiyamaShapeCone: DBH incosistent: DBH:%lf != DBH
by r(h):%lf\n",
			DBH, DBHcone);
	}
//	printf("komiyamaShapeCone: H:
%.2lf\tDBH:%.2lf\ta:%lf\tb:%lf\n",H,DBH,*a,*b);
	return 0;

}

double volumeCone( double H, double DBH, double D0 )
{
	double acon, bcon;

	acon = (DBH-D0)/2/BH;
	bcon = D0/2;

	return PAI*(acon*acon/3.*H*H*H+acon*bcon*H*H+bcon*bcon*H);
}

double findConeD0( double H, double DBH )
{
	double a, b, c, D, D0;
	double x1, x2;

	a = H*H*H/12./BH/BH - H*H/4./BH + H/4.;
	b = -DBH/6./BH/BH*H*H*H + DBH/4./BH*H*H;
	c = DBH*DBH/12/BH/BH*H*H*H -C * pow(DBH*DBH*H, alpha);

	D = b*b - 4.0*a*c;
	if( D < 0. ){
		printf("findConeD0: D<0\n");
		exit(1);
	}

	x1 = ( -b+sqrt(D) ) / 2 / a;
```

```
        x2 = ( -b-sqrt(D) ) / 2 / a;

        printf("findConeD0 %lf %lf\n", x1, x2 );
        printf("findConeD0 %lf\n", a*x1*x1+b*x1+c );
        printf("findConeD0 %lf\n", a*x2*x2+b*x2+c );

        printf("findCondD0: r at the top for x1:%lf and x2:%lf\n", rcone(H, DBH,
x1),rcone(H, DBH, x2));
        D0 = x1;
        if( rcone(H, DBH, D0) < 0 ) {
                D0 = x2;
                if( rcone(H, DBH, D0) < 0 ) {
                        printf("findConeD0: r at the top is negative to both of the
solution\n");
                }
        }

        return x2;
}

double rcone(double h, double DBH, double D0)
{
        double acon, bcon;

        acon = (DBH-D0)/2/BH;
        bcon = D0/2;

        return acon*h+bcon;

}
```